Journal of Neurochemistry JNC

JOURNAL OF NEUROCHEMISTRY | 2010 | 114 | 1840–1851 doi: 10.1111/j.1471-4159.2010.06893.x

Chronic restraint stress impairs neurogenesis and hippocampus-dependent fear memory in mice: possible involvement of a brain-specific transcription factor Npas4

Jaesuk Yun,*,[1] Hiroyuki Koike,*,†,[1] Daisuke Ibi,* Erika Toth,* Hiroyuki Mizoguchi,‡ Atsumi Nitta,* Masanori Yoneyama,§ Kiyokazu Ogita,§ Yukio Yoneda,† Toshitaka Nabeshima,¶ Taku Nagai* and Kiyofumi Yamada*,**

*Department of Neuropsychopharmacology and Hospital Pharmacy, Nagoya University Graduate School of Medicine, Nagoya, Japan
†Laboratory of Molecular Pharmacology, Graduate School of Natural Science and Technology, Kanazawa University, Kanazawa, Japan
‡Futuristic Environmental Simulation Center, Research Institute of Environmental Medicine, Nagoya University, Nagoya, Japan
§Department of Pharmacology, Faculty of Pharmaceutical Sciences, Setsunan University, Osaka, Japan
¶Department of Chemical Pharmacology, Graduate School of Pharmaceutical Sciences, Meijo University, Nagoya, Japan
**CREST, JST, Nagoya, Japan

Abstract

Neurogenesis in the hippocampus occurs throughout life in a wide range of species and could be associated with hippocampus-dependent learning and memory. Stress is well established to seriously perturb physiological/psychological homeostasis and affect hippocampal function. In the present study, to investigate the effect of chronic restraint stress in early life on hippocampal neurogenesis and hippocampus-dependent memory, 3-week-old mice were subjected to restraint stress 6 days a week for 4 weeks. The chronic restraint stress significantly decreased the hippocampal volume by 6.3% and impaired hippocampal neurogenesis as indicated by the reduced number of Ki67-, 5-bromo-2′-deoxyuridine- and doublecortin-positive cells in the dentate gyrus. The chronic restraint stress severely impaired hippocampus-dependent contextual fear memory without affecting hippocampus-independent fear memory. The expression level of brain-specific transcription factor neuronal PAS domain protein 4 (Npas4) mRNA in the hippocampus was down-regulated by the restraint stress or by acute corticosterone treatment. Npas4 immunoreactivity was detected in progenitors, immature and mature neurons of the dentate gyrus in control and stressed mice. Our findings suggest that the chronic restraint stress decreases hippocampal neurogenesis, leading to an impairment of hippocampus-dependent fear memory in mice. Corticosterone-induced down-regulation of Npas4 expression may play a role in stress-induced impairment of hippocampal function.

Keywords: hippocampus, memory, neurogenesis, Npas4, restraint stress, transcription factor.

J. Neurochem. (2010) **114**, 1840–1851.

Stress is defined in biological systems as any condition that seriously perturbs physiological/psychological homeostasis and well known to affect the function and morphology of the hippocampus (Kim and Diamond 2002). The exact underlying cellular mechanisms that mediate the inhibitory effect of stress are largely unknown. However, stress reduces the expression of several growth factors and neurotrophic factors, such as brain-derived neurotrophic factor (BDNF), insulin-like growth factor-1, nerve growth factor, epidermal growth factor, and vascular endothelial growth factor, that can all influence neurogenesis (Lucassen *et al.* 2010).

Received March 5, 2010; revised manuscript received June 28, 2010; accepted June 30, 2010.

Address correspondence and reprint requests to Dr Kiyofumi Yamada, Department of Neuropsychopharmacology and Hospital Pharmacy, Nagoya University Graduate School of Medicine, 65 Tsurumai-cho, Showa-ku, Nagoya 466-8560, Japan.
E-mail: kyamada@med.nagoya-u.ac.jp

[1]These authors contributed equally to this study.

Abbreviations used: BDNF, brain-derived neurotrophic factor; BrdU, 5-Bromo-2′-deoxyuridine; DCX, doublecortin; DG, dentate gyrus; GCL, granule cell layer; GFAP, glial fibrillary acidic protein; NeuN, neuronal nuclei; Npas4, neuronal PAS domain protein 4; PBS, phosphate-buffered saline; SGZ, subgranular zone; Sox-2, SRY-related HMG box 2.

A variety of stress paradigms also impair hippocampal neurogenesis (Mirescu and Gould 2006). Neurogenesis in the hippocampus occurs throughout life in a wide range of species (Kempermann *et al.* 1997; Eriksson *et al.* 1998). The newly divided cells in the subgranular zone (SGZ) of the dentate gyrus (DG) in the hippocampus migrate into the granule cell layer (GCL) of the DG and are integrated into the existing circuitry (Tashiro *et al.* 2006). Impairment of hippocampal neurogenesis could be one of the etiological factors for neuropsychiatric disorders (Reif *et al.* 2006), and hippocampal neurogenesis may be a target for the treatment of depression (Airan *et al.* 2007).

Recently, we have demonstrated that rearing in long-term social isolation after weaning impaired hippocampal neurogenesis and spatial memory in Morris water maze, and reduced expression levels of neuronal PAS domain protein 4 (*Npas4*) mRNA in the DG of the hippocampus (Ibi *et al.* 2008). Npas4 is a brain-specific transcription factor and may have a neuroprotective function (Ooe *et al.* 2009). It has been reported that Npas4 regulates the expression of drebrin, which engages in dendritic-cytoskeleton modulation at synapses in the hippocampus (Ooe *et al.* 2004). Recently, Npas4 has been shown to control GABAergic synapse development through the transcriptional regulation of BDNF (Lin *et al.* 2008). However, it remains to be determined whether Npas4 gene expression in the hippocampus is affected by deleterious stress. In this study, we investigated the effect of chronic restraint stress in early life on hippocampal neurogenesis, hippocampus-dependent memory and Npas4 expression in mice.

Materials and methods

Animals

Male ICR mice (3 weeks old) were purchased from Japan SLC Inc. (Hamamatsu, Japan). They were housed 5–6 per cage under standard conditions (23 ± 1°C, 50 ± 5% humidity), with a 12-h light/dark cycle. Food and water were available *ad libitum*. The animals were handled in accordance with the guidelines established by the Institutional Animal Care and Use Committee of Nagoya University.

Restraint stress procedure

Mice were randomly divided into two groups, restraint stress and control groups. Chronic stress was applied for 4 weeks with a stainless mesh that allowed for a close fit to mice (6 h/day between 10 AM and 4 PM, 6 days a week) as described previously (Takuma *et al.* 2007). For acute restraint stress, mice were subjected to the stress for 2 h or 6 h.

Corticosterone level measurement

Corticosterone levels were measured with an enzymatic immunoassay kit (Cayman, Ann Arbor, MI, USA) following the manufacturer's manual with modifications. Briefly, mice were decapitated and 1 mL of blood was collected with 30 μL of 100 mM EDTA immediately after the final restraint stress. Samples were centrifuged (15 min, 1000 *g*, 4°C). Each supernatant was added to a 96-well plate at two dilutions (1 : 150 and 1 : 300) in duplicate and subjected to the immunoassay. The optical density of the enzyme products was read at 405 nm.

Conditioned-fear test

The conditioned-fear test was carried out as described previously (Nagai *et al.* 2003). One day after the chronic stress, freezing response was measured in a neutral cage (30 cm × 30 cm × 35 cm high) for 1 min without sound (pre-conditioning phase). In the conditioning phase, each mouse was placed in a training cage (25 cm × 30 cm × 11 cm high) and allowed to explore freely for 2 min, and then a 15-s tone (85 dB) was delivered (conditioned stimulus). During the last 5 s of the tone stimulus, a foot shock of 0.8 mA was presented as an unconditioned stimulus through a shock generator (four times with 15-s intervals.). Context-dependent test was carried out 24 h after the conditioning and the tone-dependent test was conducted 3 h after the context-dependent test. For the context-dependent test, freezing behavior was measured in the training cage for 2 min without tone or foot shock presentation. For the tone-dependent test, the freezing behavior was measured in the neutral cage for 1 min in the presence of a continuous-tone stimulus. After the test phase, the sensitivity to the foot shock was determined. The foot shock was gradually increased in 0.05 mA increments until vocalization.

Nissl staining

Coronal sections (10 μm) through the entire extent of the hippocampus were cut and every fifteenth section was collected. The sections were dehydrated through an ascending series of ethanol concentrations. After dissolving lipids in xylene, they were rehydrated through a series of graded ethanol solutions. They were stained with 1% cresyl violet, differentiated in 70% ethanol containing anhydrate acetic acids and then dehydrated with 95% and 100% ethanol. Samples were observed with a microscope (Model Axioskop, Zeiss, Jena, Germany). To estimate total pyramidal and granule cell numbers, photographs (12 per section) were randomly taken from the hippocampus at a magnification of ×400, and the stained cells were counted within an 80 × 80 μm dissector frame using image-analyzing software Win ROOF (ver. 5.6, Mitani Co., Fukui, Japan). To estimate the volume of the entire hippocampus, the Cavalieri principle was used (Reilly *et al.* 2003). The hippocampal structure was outlined and the computed areas were then summed and multiplied with the thickness and with the intersection distance.

5-Bromo-2′-deoxyuridine labeling

To measure the effect of chronic restraint stress on survival and differentiation of newly divided cells in the DG, 5-bromo-2′-deoxyuridine (BrdU) labeling was carried out 1 day before starting the chronic restraint stress. BrdU was purchased from Sigma-Aldrich (St Louis, MO, USA) and dissolved in saline. BrdU (75 mg/kg) was injected intraperitoneally (i.p.) three times at 2-h intervals as described previously (Ibi *et al.* 2008).

Immunohistochemistry

After stress, mice were deeply anesthetized with diethyl ether, and transcardially perfused with ice-cold saline followed by 4% parafor-

maldehyde in 0.1 M phosphate-buffered saline (PBS, pH 7.4). The brain was post-fixed in the same fixative and cryoprotected in 0.1 M PBS (30% sucrose). The brain was embedded in Tissue-Tek O.C.T. compound (Sakura Finetech, Tokyo, Japan) and stored at −80°C. Every fifth coronal section (30 μm) was collected between stereotaxic coordinates bregma −1.2 to 3.0 according to the brain atlas (Paxinos and Franklin 2004). For BrdU single-staining, sections were treated with 0.1% Nonidet-40/0.01 M PBS (pH 7.4) overnight (4°C) and denatured in a microwave oven in 0.01 M citrate buffer (pH 6.0). After blocking in 10% goat serum/PBS with 0.1% Nonidet-40 (Sigma-Aldrich), BrdU-positive cells in the sections were detected using BrdU labeling and detection kit 2 (Roche Diagnotics GmbH, Mannheim, Germany) according to the manufacturer's instructions. For double-staining of BrdU/neuronal nuclei (NeuN) and BrdU/glial fibrillary acidic protein (GFAP), sections were pre-treated with 1 M HCl, followed by 0.1 M borate buffer and then washed in PBS before blocking. Rat anti-BrdU antibody (1 : 200; Abcam, Cambridge, UK), mouse anti-NeuN antibody (1 : 100; Millipore, Billerica, MA, USA) and mouse anti-GFAP antibody (1 : 1500; Sigma-Aldrich) diluted in PBS (0.1% Triton X-100 and 5% goat serum) were applied to sections [overnight, 4°C and 6 h, room temperature (RT)]. After washing, goat anti-rat Alexa 568 and goat anti-mouse Alexa 488 (1 : 1000; Invitrogen, Eugene, OR, USA) antibodies were applied to sections (2 h, 25°C). For Ki67 or doublecortin (DCX) single-staining, sections were treated with 0.5% hydrogen peroxide in methanol to block endogenous peroxidase activity, and denatured in the microwave oven. They were incubated in blocking solution (10% goat serum and 0.1% Triton X-100 in 0.01 M PBS, 1 h), and then with rabbit anti-Ki67 (1 : 2000; Novocastra, Newcastle, UK) or rabbit anti-DCX (1 : 500; Abcam) antibody (overnight, 4°C). They were washed and incubated with biotinylated goat anti-rabbit antibody (1 : 200; Vector Laboratories, Burlingame, CA, USA, 1 h, 25°C). The sections were washed and processed with avidin-biotinylated horseradish peroxidase complex (Vector ABC kit, Vector Laboratories), and the reaction was visualized using diaminobenzidine. For double-staining of Npas4/several cell markers, coronal sections (10 μm) were incubated with blocking solution (3% bovine serum albumin, 10% donkey serum and 0.3% Triton X-100 in 0.01 M PBS, 1 h, 25°C), and then with primary antibodies (overnight, 4°C). They were washed with 0.01 M PBS and incubated with secondary antibodies (2 h, 25°C). Sections were mounted in fluorescent medium (S3023; Dako Cytomation, Kyoto, Japan). The following antibodies were used: rabbit anti-Npas4 (1 : 32), mouse anti-NeuN (1 : 200; Millipore), mouse anti-Calbindin D-28 (1 : 500; Swant, Bellinzona, Switzerland), goat anti-DCX (1 : 50; Santa Cruz Biotechnology, Santa Cruz, CA, USA), goat anti-Sox-2 (1 : 100; Santa Cruz Biotechnology), Alexa 488-conjugated donkey anti-rabbit (1 : 500, Invitrogen), Alexa 594-conjugated goat anti-mouse (1 : 500, Invitrogen) and Alexa 594-conjugated donkey anti-goat (1 : 500, Invitrogen). The rabbit anti-Npas4 antibody (Japan Bio Services Co., Ltd., Saitama, Japan) was raised against a carboxy-terminal region of Npas4 (amino acids 622–635). For pre-absorption experiment, Npas4 antibody was incubated with a 5-fold excess of the antigen peptide (overnight, 4°C).

Quantification of immunostaining cells

Every fifth section throughout the hippocampus (total 12 sections from each mouse) was processed for BrdU, Ki67 and DCX immunohistochemistry. All immunostained cells in DG were examined using a light microscope (Axio Imager; Zeiss) and counted by a blind experimenter. All counts were performed at 400× magnification (objective; 40×). To obtain the total number of cells per DG, we multiplied the counted number of positive cells by five. Double-stained cells were imaged and quantified using a confocal laser scanning microscope (LSM 510; Zeiss). Each cell was analyzed along the entire '*z*' axis. Ratios of BrdU-positive cells co-labeled with NeuN or GFAP among BrdU-positive cells were determined.

Quantitative analyses of Npas4 mRNA by real-time RT-PCR

Mice were decapitated and brains were removed immediately after restraint stress or 4 h after corticosterone injection (10 mg/kg, s.c., in corn oil, Sigma-Aldrich). For DG, tissues from two animals were pooled as one sample and for hippocampus tissue from one animal used as one sample. The total RNA isolated from the DG or hippocampus (RNeasy Mini Kit, Qiagen, Hilden, Germany) was converted into cDNA using SuperScript III First-Strand Synthesis System for RT-PCR (Invitrogen) and quantified using a 7300 real-time PCR System (Applied Biosystems, Foster City, CA, USA). Quantitative real-time RT-PCR was performed in a volume of 25 μL with 0.5–1.0 μg of cDNA and 0.5 μM primers in the Power SYBR Green Master Mix (Applied Biosystems). The primers used were as follows: 5′-AGCATTCCAGGCTCATCTGAA-3′ (forward) and 5′-GGCGAAGTAAGTCTTGGTAGGATT-3′ (reverse) for Npas4, 5′-TGTCAAGCTCATTTCCTGGTATGA-3′ (forward) and 5′-CTTACTCCTTGGAGGCCATGTAG -3′ (reverse) for glyceraldehyde-3-phosphate dehydrogenase, 5′-CGATGCCCTGAGGCTCTTT-3′ (forward) and 5′-TGGATGCCACAGGATTCCA -3′ (reverse) for β-actin used as internal controls.

In situ hybridization

Npas4 mRNA level in tissue was detected with an *in situ* hybridization kit (Nippongene, Tokyo, Japan) following the manufacturer's manual with modifications. Briefly, immediately after restraint stress, mice were deeply anesthetized with diethyl ether, and transcardially perfused with ice-cold saline followed by 4% paraformaldehyde in 0.1 M PBS (pH 7.4). The brains were removed, post-fixed in the same fixative and then cryoprotected in 12%, 15% and 18% sucrose in Hanks' Balanced Salt Solution (HBSS) buffer (pH 7.4). The brains were embedded in Tissue-Tek O.C.T. compound (Sakura Finetech) and stored at −80°C. Thick coronal brain sections of 10 μm were cut and mounted. Nucleotides 1485–2409 of Npas4 (BC_129861) were used as a template for transcription and labeling of Npas4 antisense and sense with digoxigenin-UTP (Roche Diagnotics GmbH). Sections were hybridized with probes and mRNA signals were visualized by enzyme-catalyzed color reaction with an NBT/BCIP kit (Roche Diagnotics GmbH, 16 h, 25°C) in a dark room.

Statistical analysis

Statistical analyses were performed using SigmaStat 3.1 software (Systat Software, Inc., Chicago, IL, USA). For body weight gain, differences among groups were analyzed by repeated measures ANOVA. Differences among groups were analyzed by Student's *t*-test or one-way ANOVA, followed by Bonferroni's *post hoc* test.

Results

Effect of chronic restraint stress on body weight gain and blood corticosterone level, hippocampal volume and the number of Nissl-stained cells in the hippocampus

To explore whether the mice that received 4-week chronic restraint stress revealed biologically significant features, we measured stress responses during and after the stress. During the period of 4 weeks of stress, chronic restraint stress significantly inhibited the body weight gain [0 day, control group, 19.5 ± 0.1 g; stress group, 19.7 ± 0.1 g; 24th day, control group, 40.1 ± 0.4 g; stress group, 31.9 ± 0.7 g, treatment, F (1, 21) = 165.719, $p < 0.001$; days, F (8, 168) = 717.763, $p < 0.001$; treatment and day interaction, F (8, 168) = 41.147, $p < 0.001$, Fig. 1a]. Blood corticosterone level after the final restraint stress was significantly increased in stressed mice compared with that of the control group ($p < 0.05$, Fig. 1b). To determine whether chronic restraint stress influences hippocampal volume and the number of hippocampal cells, we performed Nissl staining. Chronic restraint stress significantly decreased the hippocampal volume by 6.3% ($p < 0.05$), but there was no significant difference in the number of Nissl-stained cells in the hippocampus (Table 1, Figure S1).

Effect of chronic restraint stress on associative fear memory

Mice were subjected to the conditioned fear memory test to examine the function of hippocampus after chronic restraint stress for 4 weeks. Contextual fear memory requires both amygdala and hippocampus (Phillips and LeDoux 1992; Anagnostaras *et al.* 1999), whereas tone-dependent memory requires the amygdala but not the hippocampus. In the context-dependent test, mice were returned to the conditioning box, and then their freezing behavior was analyzed for 2 min. The mice subjected to chronic restraint stress exhibited significantly less freezing behavior than control mice ($p < 0.05$, Fig. 1c). On the other hand, there was no significant difference in freezing time between control and stressed mice when the freezing behavior was analyzed in the neutral cage in the presence of a continuous-tone stimulus identical to the conditioned stimulus (Fig. 1d). Mice were tested for foot shock threshold to be sure that any alterations in memory were not because of changes in sensitivity to foot shock. There was no significant difference in the pain threshold of the chronic stress mice (0.27 ± 0.02 mA, n = 16) compared with that of the control mice (0.29 ± 0.02 mA, n = 16).

Effect of chronic restraint stress on hippocampal neurogenesis

As recent studies have suggested that neurogenesis plays an important role in hippocampus-dependent memory (Leuner *et al.* 2006; Imayoshi *et al.* 2008; Kitamura *et al.* 2009) and chronic restraint stress exposure led to memory deficit in a hippocampus-dependent manner, we examined the effect of chronic restraint stress on cell proliferation in the DG of the hippocampus. Ki67-positive cells, for which the antigen is expressed in all active parts of the cell cycle, G1, S, G2 and

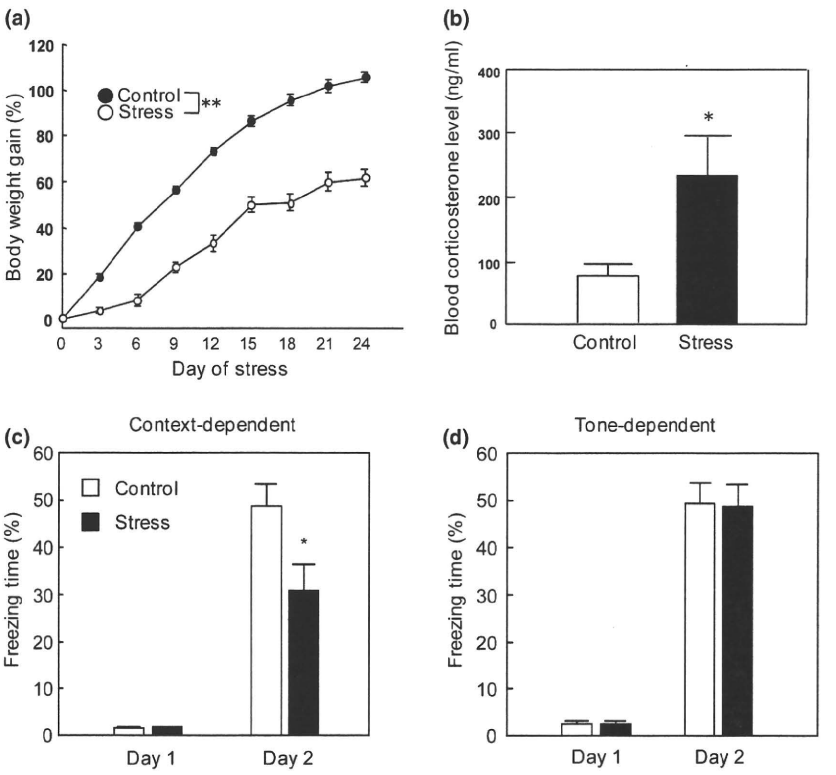

Fig. 1 Effect of chronic restraint stress on body weight gain, blood corticosterone level and fear memory. (a) Chronic restraint stress inhibits body weight gain. Body weight gain is expressed as a percentage of that at day 0. Values indicate the means ± SE (n = 11–12). (b) Chronic restraint stress increases the blood corticosterone level. Values indicate the means ± SE (n = 6). (c) Chronic restraint stress decreases context-dependent memory. (d) Tone-dependent test results do not reveal any significant difference between control and stressed mice. Values indicate the means ± SE (n = 16). *$p < 0.05$ vs. control (Student's t-test), **$p < 0.001$ between groups (repeated measures ANOVA).

Table 1 Effect of chronic restraint stress on the hippocampal volume and Nissl-stained cell number in hippocampal CA1, CA3 and dentate gyrus

Group	Hippocampal volume (mm^3)	Nissl-stained cells ($\times 10^2$ counts/mm^2)		
		CA1	CA3	DG
Control	6.98 ± 0.17	42.01 ± 0.53	40.64 ± 1.42	119.96 ± 1.24
Stress	6.54 ± 0.11*	41.50 ± 1.03	37.64 ± 1.19	115.55 ± 2.1

Values indicate the means ± SE ($n = 8$). *$p < 0.05$ vs. control (Student's *t*-test).

M (mitosis) phases but not G0 phase (Braun *et al.* 1988), were mainly observed in the SGZ rather than other areas as either clusters or single cells (Fig. 2a). Chronic restraint stress significantly decreased the number of Ki67-positive cells in the SGZ by 17% ($p < 0.05$) and thereby reduced that in the DG by 16% ($p < 0.05$, Table 2).

5-Bromo-2′-deoxyuridine is incorporated into the DNA of proliferating cells during the S phase of the cell cycle (Rakic 2002) and has been utilized in a number of *in vitro* and *in vivo* studies to label neural progenitors. To measure the effect of chronic restraint stress on the survival of newly divided cells in the DG, BrdU was injected into mice 1 day before the chronic restraint stress was initiated, and the numbers of BrdU-positive cells were counted after 4 weeks of restraint stress. There was an apparent difference between control and stressed mice in the number and location of BrdU-positive cells in the DG of hippocampus (Fig. 2b). Chronic restraint stress significantly decreased the number of BrdU-positive cells in the GCL by 27% ($p < 0.01$) and thereby decreased that in the DG by 32% ($p < 0.05$, Table 2). DCX is one of the immature granule neuron markers and is useful to assess the rate of neurogenesis in the adult mammalian hippocampus (Liu *et al.* 2008). Chronic restraint stress significantly decreased the number of DCX-positive cells in the SGZ by 13% ($p < 0.05$) and thereby decreased that in the DG by 13% ($p < 0.05$, Fig. 2c, Table 2).

Finally, we investigated the effect of chronic restraint stress on the differentiation of newly divided cells. Mice were subjected to 4-week chronic restraint stress after BrdU injection, and then we measured NeuN-positive cells (neuron) and GFAP-positive cells (astrocyte) among BrdU-labeled cells in the DG of the hippocampus. There was no apparent difference in the distribution and the rate

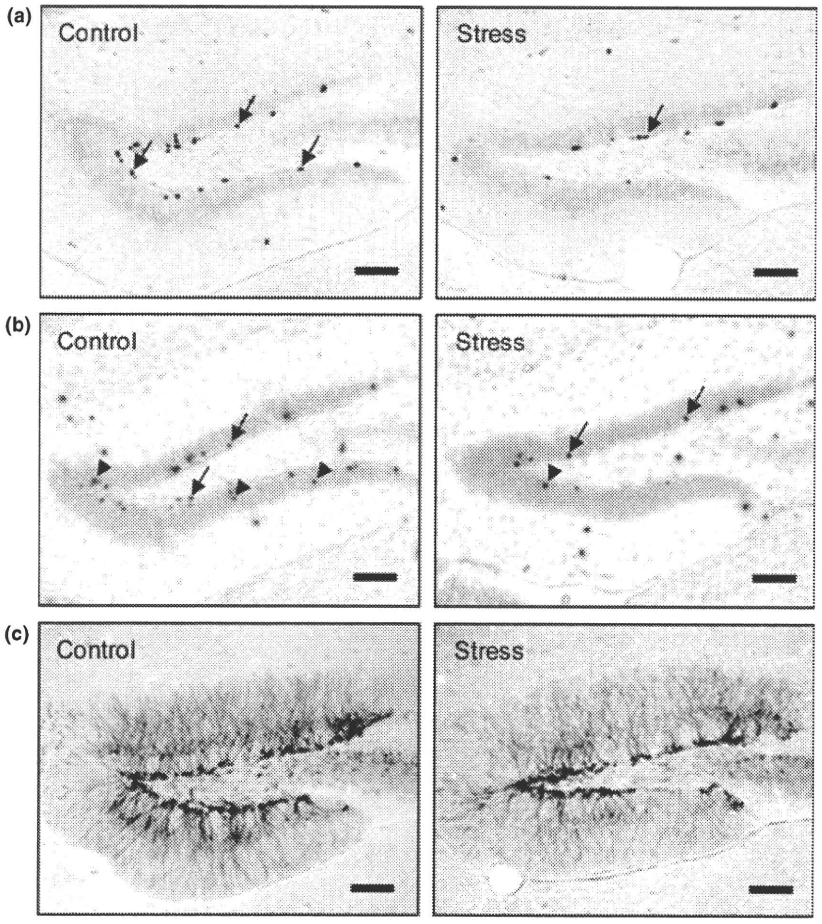

Fig. 2 Effect of chronic restraint stress on the number of Ki67-positive cells, the survival of BrdU-positive newly divided cells and the number of doublecortin (DCX)-positive cells in the dentate gyrus of hippocampus. (a) Representative photographs showing the distribution of Ki67-positive cells in control (left) and stress (right) mice. (b) Representative photographs showing the distribution of BrdU-positive cells in control (left) and stress (right) mice. (c) Representative photographs showing the distribution of DCX-positive cells in control (left) and stress (right) mice. Scale bar: 100 μm.

Table 2 Effect of chronic restraint stress on the number of Ki67-positive cells, the survival of BrdU-positive newly divided cells and the number of doublecortin (DCX)-positive cells in the dentate gyrus of hippocampus

	Control group				Stress group			
	Total	Hilus	GCL	SGZ	Total	Hilus	GCL	SGZ
Ki67	2628.3 ± 77.0	177.5 ± 19.0	259.2 ± 49.8	2191.7 ± 64.4	2200.0 ± 150.6*	129.2 ± 16.1	252.5 ± 28.4	1818.3 ± 136.1*
BrdU	1241.0 ± 107.9	134.8 ± 12.3	792.8 ± 74.5	313.5 ± 33.7	895.2 ± 49.7*	118.1 ± 9.7	533.9 ± 43.8**	243.2 ± 26.2
DCX	11 555.1 ± 479.2	33.5 ± 11.9	1271.7 ± 173.3	10 249.9 ± 309.8	9993.3 ± 327.0*	36.7 ± 10.7	1090.8 ± 170.1	8865.8 ± 343.0*

Total numbers of cells are expressed as the sum of the number in the SGZ, hilus and GCL. Values indicate the means ± SE (n = 6–10). *$p < 0.05$, **$p < 0.01$ vs. control (Student's t-test).

of NeuN- (Fig. 3a and b) or GFAP-positive cells (Fig. 3a and c) among BrdU-labeled cells in the DG of the hippocampus.

Effect of restraint stress on the expression levels of Npas4 mRNA in the dentate gyrus

To address whether restraint stress reduces Npas4 expressions in the DG of the hippocampus, mice were subjected to acute (2 h or 6 h) or chronic (6 h/day, 6 days a week for 4 weeks) restraint stress. The expression levels of Npas4 mRNA in the DG were analyzed by real-time RT-PCR. Both acute (2 h and 6 h) and chronic restraint stresses significantly decreased the levels of Npas4 mRNA compared with those in control mice [F (3, 16) = 8.718, p = 0.01, Fig. 4a]. *In situ* hybridization analysis revealed that intense signals that react with antisense Npas4 probes were detected in the pyramidal and granule cell layer in the hippocampus. There was no signal detected when sense probes were used, suggesting that Npas4 mRNA is abundant in the hippocampus (Fig. 5a). Chronic restraint stress markedly decreased the signals of Npas4 mRNA in the DG, CA3 and CA1 subregions of the hippocampus compared with those in control mice (Fig. 5b).

Effect of corticosterone treatment on the expression levels of Npas4 mRNA in the hippocampus

To address the relationship among stress exposure, reduction of Npas4 expression and the stress-induced impairment of neurogenesis and hippocampus-dependent fear memory, we examined the effect of corticosterone injection in mice on Npas4 mRNA levels in the hippocampus. The Npas4 mRNA levels in the hippocampus of mice following corticosterone injection were significantly reduced to 70.0% ($p < 0.05$) that of vehicle-treated control mice (Fig. 4b).

Phenotype of Npas4-positive cells in the dentate gyrus of the hippocampus

Finally, to characterize the Npas4-expressing cells in the DG, we performed double immunostaining for Npas4 and several cell markers such as SRY-related HMG box 2 (Sox-2), DCX, calbindin and NeuN. Antibody pre-absorption with the antigen peptide completely blocked the Npas4 staining in the DG (Figure S2). Sox-2 is a marker for both quiescent neural progenitors and amplifying neural progenitors (Segi-Nishida *et al.* 2008). DCX is a marker for immature neurons, while calbindin and NeuN are mature neural markers in the DG. At 7 weeks old, most Npas4 immunoreactivities were co-localized with the cells positive for NeuN in the GCL of control mice (Figs 6a and S2), while some of them partially co-localized with the cells positive for Sox-2 (Figs 6b and S2), DCX (Figs 6c and S2) in the SGZ and calbindin in the GCL (Figs 6d and S2). Similar results were observed in the stressed mice (Figs 6e–h and S2). Immunoblot studies revealed that the protein expression level of Npas4 in DG was not changed significantly in stressed mice (data not shown).

Discussion

We demonstrated in the present study that chronic restraint stress after weaning decreased cell proliferation, survival of newly divided cells and neurogenesis in the DG. Numerous studies have reported that stress disrupts hippocampal neurogenesis. Cell proliferation in the DG is decreased by a variety of stress paradigms, including restraint stress (Nagata *et al.* 2009; Veena *et al.* 2009), subordination stress (Yap *et al.* 2006), social isolation (Dong *et al.* 2004), resident-intruder stress (Gould *et al.* 1998), water immersion restraint stress (Tamaki *et al.* 2008), chronic unpredictable stress (Heine *et al.* 2004), predator odor (Mirescu *et al.* 2004), sleep deprivation (Mirescu *et al.* 2006) and chronic mild stress (Alonso *et al.* 2004). Otherwise, the effect of stress on survival and differentiation of newly divided cells is more intricate than cell proliferation. Several studies have shown that the decrease of cell proliferation in the DG results in the suppression of neuronal generation (Pham *et al.* 2003; Westenbroek *et al.* 2004). Other reports have indicated that the influence of stress on hippocampal neurogenesis is very short-lived, and the decrease in the number of neuronal precursor cells is followed by an enhancement of cell survival, as the total number of new mature neurons appears unchanged (Tanapat *et al.* 2001; Malberg and Duman 2003).

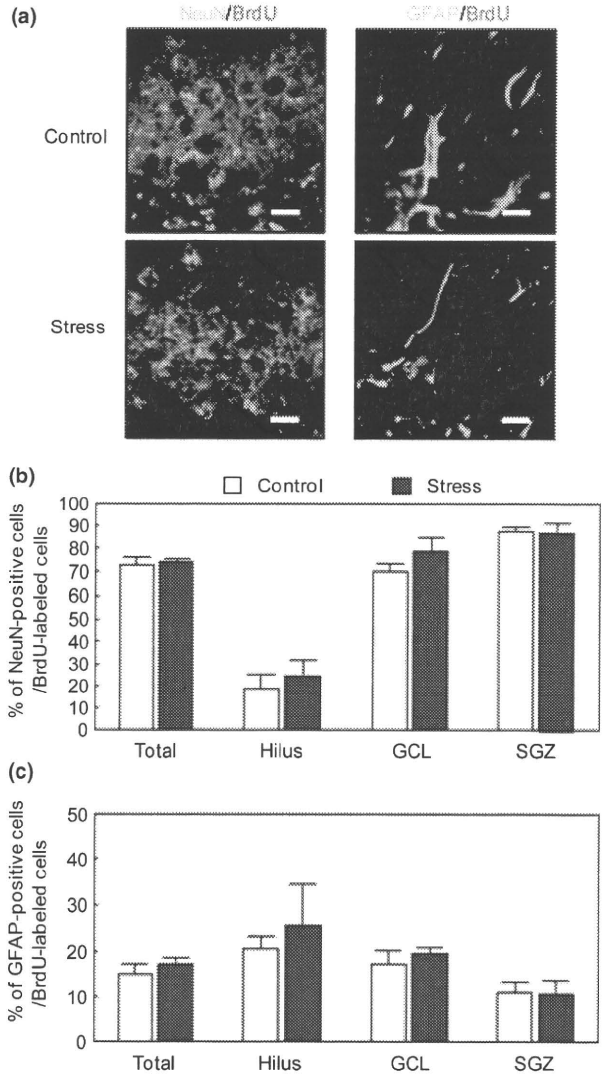

Fig. 3 Effect of chronic restraint stress on the percentage of NeuN-positive cells and GFAP-positive cells among BrdU-labeled cells in the dentate gyrus of the hippocampus. (a) Representative photographs showing confocal analysis at 4 weeks after BrdU and NeuN or GFAP double staining (NeuN, GFAP: green; BrdU: red; double-stained cells: yellow). Scale bar: 10 μm. (b) Percentage of neurons (NeuN-positive cells) among BrdU-labeled cells. Immunocytochemistry studies do not reveal any significant difference between control and stressed mice. Values indicate the means ± SE (n = 5). (c) Percentage of astroglial cells (GFAP-positive cells) among BrdU-labeled cells. Immunocytochemistry studies do not reveal any significant difference between control and stressed mice. Values indicate the means ± SE (n = 5).

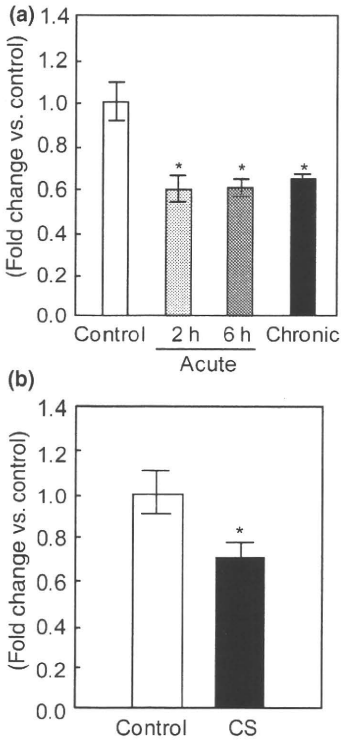

Fig. 4 Effect of restraint stress acute corticosterone treatment on the expression levels of Npas4 mRNA in the hippocampus. (a) Acute and chronic restraint stress decrease the expression levels of Npas4 mRNA in the DG of hippocampus, $^*p < 0.05$ vs. control (Bonferroni's *post hoc* test). Values indicate the means ± SE (n = 5, each from two mice). (b) Acute corticosterone (CS) injection at a dose of 10 mg/kg significantly reduces Npas4 mRNA levels in the hippocampus 4 h after the treatment, $^*p < 0.05$ vs. control (Student's t-test). Values indicate the means ± SE (n = 8–9).

On the other hand, chronic stress after BrdU labeling decreases the survival of newly divided cells (Lee *et al.* 2006; Ibi *et al.* 2008). Our current findings are generally consistent with previous studies. Indeed, the stress exposure paradigm in this study was sufficient to increase serum corticosterone level in stressed mice compared with that in control mice, which may affect the fate of newly generated neurons in the DG. Meanwhile, chronic restraint stress had no apparent effect on the distribution and the rate of NeuN- or GFAP-positive cells among BrdU-labeled cells in the DG of the hippocampus. These results suggest that differentiation of newly divided cells in the hippocampus may be unaffected by chronic restraint stress after weaning in mice; however, we should also investigate the effect of chronic restraint stress on microglial cells.

We also found that chronic restraint stress significantly decreased the hippocampal volume without affecting the number of Nissl-stained cells. It has been reported that chronic restraint stress decreased the length and branch of apical dendrites in the CA3 subregion (Watanabe *et al.* 1992; Magariños and McEwen 1995). Therefore, atrophy of the apical dendrites of CA3 pyramidal neurons and the decrease of neurogenesis in the DG may be related to the reduction of hippocampal volume.

As regards the functional changes in the hippocampus, we demonstrated that chronic restraint stress impaired context-dependent fear memory in mice. Even though there is a

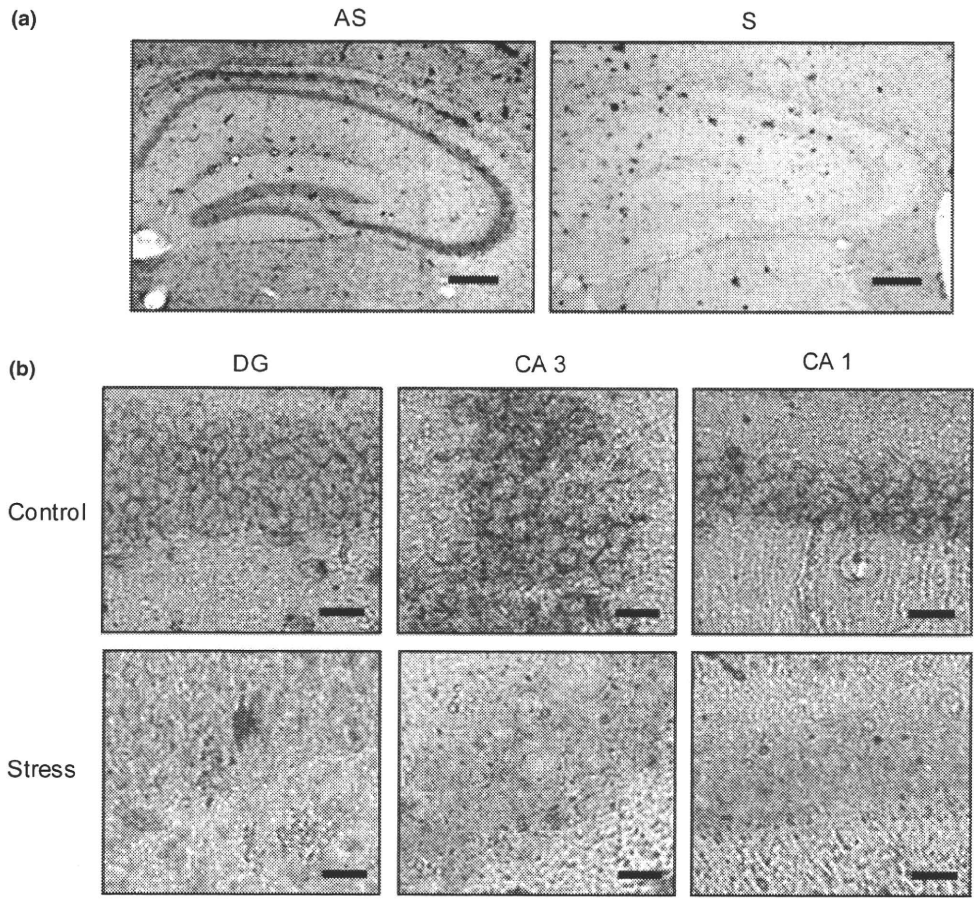

Fig. 5 Effect of chronic restraint stress on the expression of Npas4 mRNA in the hippocampus. DG (dentate gyrus), AS (antisense), S (sense). (a) Representative photographs showing *in situ* hybridization analysis of Npas4 mRNA using antisense or sense probe. Scale bar: 200 μm. (b) Chronic restraint stress (bottom) decreases Npas4 mRNA expression level in DG, CA3 and CA1 subregions of hippocampus compared with those of control (top). Scale bar: 20 μm.

report that chronic restraint stress enhanced fear memory (Conrad *et al.* 1999), it is generally accepted that stress impairs memory in rodents and the increased levels of circulating glucocorticoids inhibit memory in rodents (Lemaire *et al.* 2000; Montaron *et al.* 2006). The context-dependent fear memory is hippocampus-dependent (Phillips and LeDoux 1992) and the hippocampus is involved in acquisition and transient storage of context-dependent fear memory (Phillips and LeDoux 1992; Anagnostaras *et al.* 1999). Although a few studies have reported that contextual fear memory was not influenced by hippocampal neurogenesis (Shors *et al.* 2001; Zhang *et al.* 2008), irradiated rats or mice, ganciclovir-treated *GFAP-tk* mice and tamoxifen-treated *Nes-CreER^{T2}/NSE-DTA* mice, all of which show defects of neurogenesis in the hippocampus, are defective in the conditioned fear memory test (Winocur *et al.* 2006; Imayoshi *et al.* 2008). In contrast to the context-dependent memory, tone-dependent fear memory was not significantly affected in chronic restrained mice. It is reported that tone-dependent fear memory is hippocampus-independent, but the lateral nucleus of the amygdala links the auditory conditioned stimulus with the fear response via the thalamo-amygdala or thalamo-cortico-amygdala pathway (LeDoux *et al.* 1990; Romanski and LeDoux 1992). Taken together, our results suggest that chronic restraint stress in mice, which leads to the hypersecretion of glucocorticoids, may disrupt the hippocampal function as evidenced by the impairment of context-dependent fear conditioned memory, which is associated with the inhibition of neurogenesis in the hippocampus and reduced hippocampal volume.

To clarify the putative molecular candidates for the stress-induced memory impairment and morphological changes in the hippocampus, we examined whether the expression level of Npas4 was regulated by stress and circulating corticosterone level. Acute or chronic restraint stress exposure as well as acute corticosterone injection significantly reduced the mRNA levels of Npas4 in the DG and the hippocampus, respectively, suggesting that stress may decrease Npas4

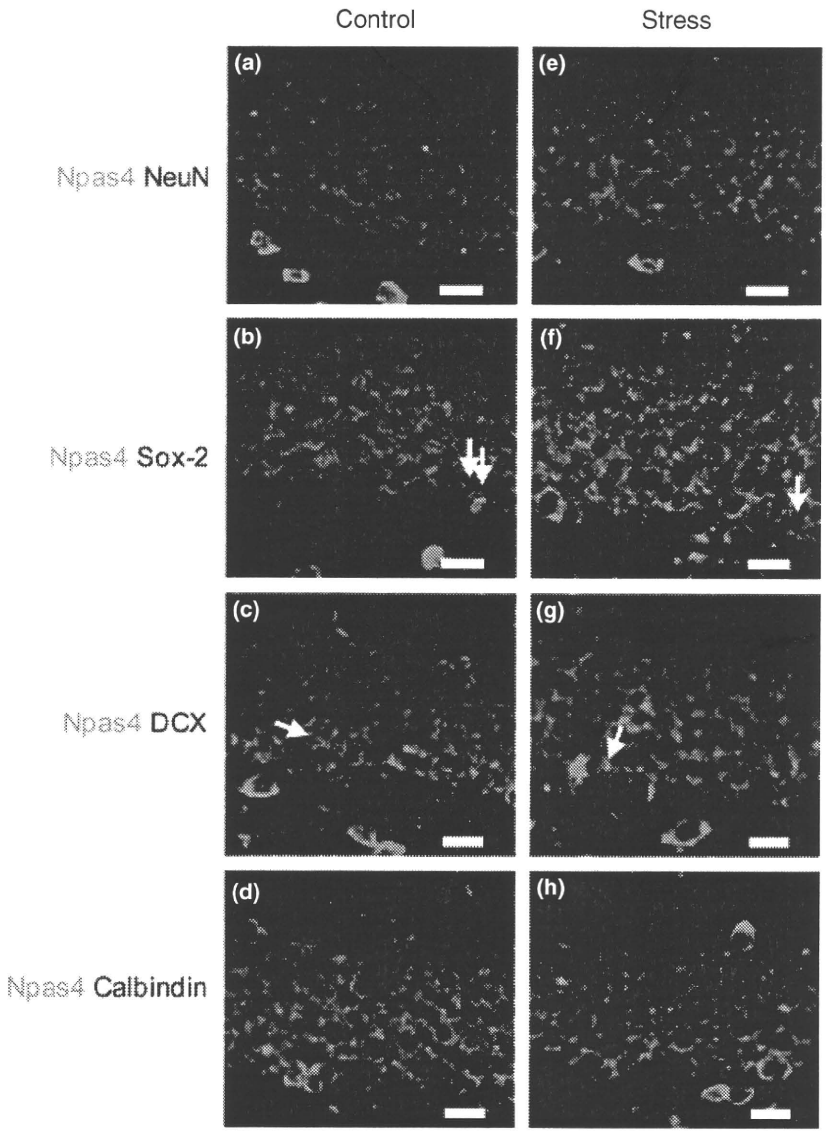

Fig. 6 Phenotype of Npas4-positive cells in the dentate gyrus (DG) of control and stressed mice. Representative photographs showing Npas4 and cell marker double staining in control (left) and stress (right) mice (Npas4: green; NeuN, Sox-2, DCX and calbindin: red; double-stained cells: yellow). (a, e) Npas4 was expressed in NeuN-positive neurons (NeuN). (b, f) Some of the neural progenitors (Sox-2-positive, arrows) expressed Npas4. (c, g) Npas4 were expressed in most immature neurons (DCX-positive, arrows). (d, h) Npas4 were expressed in most mature neurons (calbindin-positive). Scale bar: 20 μm.

expression in the hippocampus through the action of circulating corticosterone level. It has been reported that Npas4 mRNAs are highly expressed in the hippocampus (Moser *et al.* 2004). Npas4 has constitutive or developmental functions that may be critical for regulating the transcriptional control of limbic patterning and function (Moser *et al.* 2004). Npas4 plays a role in the development of inhibitory synapses by regulating the expression of activity-dependent genes and appears to regulate a wide variety of genes modulating synaptic functions (Lin *et al.* 2008). Furthermore, we observed that Npas4 mRNA is present in neural stem/progenitor cells derived from the hippocampus of embryonic mice as originally described by Yoneyama *et al.* (2007, 2009) (data not shown).

Interestingly, BDNF is a target gene of Npas4 in mouse hippocampal primary cultures (Lin *et al.* 2008), and the expression level of BDNF is reported to be decreased by stress in the hippocampus (Vaidya *et al.* 1999; Xu *et al.* 2006). It is well known that BDNF positively regulates neurogenesis and plays a role in the differentiation and survival of neuronal progenitor cells (Sairanen *et al.* 2005; Scharfman *et al.* 2005). We assume that the inhibition of Npas4 gene expression in both progenitor cells and mature neurons may contribute to the decreased action of BDNF in the hippocampus. Taken together, chronic stress may reduce Npas4 expression in the DG of hippocampus through the action of corticosterone, leading to an impairment of hippocampal neurogenesis and hippocampus-dependent memory in mice. To further support the involvement of Npas4 in stress-induced impairment of neurogenesis, we showed that Npas4 was expressed in some of the Sox-2-positive cells, and most DCX- and calbindin-positive cells

were colocalized with Npas4 in the hippocampus. These findings suggest that Npas4 is expressed from an early developmental stage of newly divided cells in the DG and that the down-regulation of Npas4 could be related to the impairment of neurogenesis by restraint stress.

Involvement of Npas4 in the hippocampal dysfunction through the impairment of neurogenesis induced by stress is also possible because neurogenesis modulates the hippocampus-dependent fear memory (Kitamura *et al.* 2009), in addition, newborn cells in adult DG may extend axons into the CA3 region, which release glutamates as their main neurotransmitter and form functional synapses with target cells (Toni *et al.* 2008). We revealed by *in situ* hybridization that stress decreased the mRNA expression level of Npas4 in DG, CA3 and CA1 subregions of hippocampus. Although we do not have any definitive evidence that the down-regulation of Npas4 mRNA expression level in CA3 and CA1 regions contributes to the reduced volume of hippocampus and impaired fear conditioned memory, Npas4 may play a role in synaptic and structural plasticity as well as hippocampal function in CA3 and CA1 regions because this transcription factor has been shown to regulate GABAergic synapse development in an activity-dependent manner (Lin *et al.* 2008) and to possibly play a role in dendritic-cytoskeleton modulation at synapses in the hippocampus (Ooe *et al.* 2004, 2009).

Acknowledgements

This study was supported in part by Grants-in-Aid for Scientific Research (Nos. 19390062 and 22390046) from the JSPS, the Global COE program from the Ministry of Education, Culture, Sports, Science and Technology of Japan, the Academic Frontier Project for Private Universities; matching fund subsidy from MEXT, 2007–2011, the Research on Risk of Chemical Substances, Health and Labour Science Research Grants supported by Ministry of Health, Labour and Welfare, Takeda Science Foundation, AstraZeneca Research Grant 2008, and JST, CREST.

Disclosure/conflicts of interest

The authors declare that there is no conflict of interest in the publication of this work.

Supporting information

Additional supporting Information may be found in the online version of this article:

Figure S1. Effect of chronic restraint stress on the Nissl-stained cell number in hippocampal CA1, CA3 and dentate gyrus.

Figure S2. Phenotype of Npas4-positive cells in the dentate gyrus (DG) of control and stressed mice.

As a service to our authors and readers, this journal provides supporting information supplied by the authors. Such materials are peer-reviewed and may be re-organized for online delivery, but are not copy-edited or typeset. Technical support issues arising from supporting information (other than missing files) should be addressed to the authors.

References

Airan R. D., Meltzer L. A., Roy M., Gong Y., Chen H. and Deisseroth K. (2007) High-speed imaging reveals neurophysiological links to behavior in an animal model of depression. *Science* **317**, 819–823.

Alonso R., Griebel G., Pavone G., Stemmelin J., Le Fur G. and Soubrie P. (2004) Blockade of CRF(1) or V(1b) receptors reverses stress-induced suppression of neurogenesis in a mouse model of depression. *Mol. Psychiatry* **9**, 278–286.

Anagnostaras S. G., Maren S. and Fanselow M. S. (1999) Temporally graded retrograde amnesia of contextual fear after hippocampal damage in rats: within-subjects examination. *J. Neurosci.* **19**, 1106–1114.

Braun N., Papadopoulos T. and Müller-Hermelink H. K. (1988) Cell cycle dependent distribution of the proliferation-associated Ki-67 antigen in human embryonic lung cells. *Virchows Arch B Cell Pathol. Incl. Mol. Pathol.* **56**, 25–33.

Conrad C. D., LeDoux J. E., Magariños A. M. and McEwen B. S. (1999) Repeated restraint stress facilitates fear conditioning independently of causing hippocampal CA3 dendritic atrophy. *Behav. Neurosci.* **113**, 902–913.

Dong H., Goico B., Martin M., Csernansky C. A., Bertchume A. and Csernansky J. G. (2004) Modulation of hippocampal cell proliferation, memory, and amyloid plaque deposition in APPsw (Tg2576) mutant mice by isolation stress. *Neuroscience* **127**, 601–609.

Eriksson P. S., Perfilieva E., Björk-Eriksson T., Alborn A. M., Nordborg C., Peterson D. A. and Gage F. H. (1998) Neurogenesis in the adult human hippocampus. *Nat. Med.* **4**, 1313–1317.

Gould E., Tanapat P., McEwen B. S., Flügge G. and Fuchs E. (1998) Proliferation of granule cell precursors in the dentate gyrus of adult monkeys is diminished by stress. *Proc. Natl Acad. Sci. USA* **95**, 3168–3171.

Heine V. M., Maslam S., Zareno J., Joëls M. and Lucassen P. J. (2004) Suppressed proliferation and apoptotic changes in the rat dentate gyrus after acute and chronic stress are reversible. *Eur. J. Neurosci.* **19**, 131–144.

Ibi D., Takuma K., Koike H. *et al.* (2008) Social isolation rearing-induced impairment of the hippocampal neurogenesis is associated with deficits in spatial memory and emotion-related behaviors in juvenile mice. *J. Neurochem.* **105**, 921–932.

Imayoshi I., Sakamoto M., Ohtsuka T., Takao K., Miyakawa T., Yamaguchi M., Mori K., Ikeda T., Itohara S. and Kageyama R. (2008) Roles of continuous neurogenesis in the structural and functional integrity of the adult forebrain. *Nat. Neurosci.* **11**, 1153–1161.

Kempermann G., Kuhn H. G. and Gage F. H. (1997) More hippocampal neurons in adult mice living in an enriched environment. *Nature* **386**, 493–495.

Kim J. J. and Diamond D. M. (2002) The stressed hippocampus, synaptic plasticity and lost memories. *Nat. Rev. Neurosci.* **3**, 453–462.

Kitamura T., Saitoh Y., Takashima N., Murayama A., Niibori Y., Ageta H., Sekiguchi M., Sugiyama H. and Inokuchi K. (2009) Adult neurogenesis modulates the hippocampus-dependent period of associative fear memory. *Cell* **139**(4), 814–827.

LeDoux J. E., Cicchetti P., Xagoraris A. and Romanski L. M. (1990) The lateral amygdaloid nucleus: sensory interface of the amygdala in fear conditioning. *J. Neurosci.* **10**, 1062–1069.

Lee K. J., Kim S. J., Kim S. W. *et al.* (2006) Chronic mild stress decreases survival, but not proliferation, of new-born cells in adult rat hippocampus. *Exp. Mol. Med.* **38**, 44–54.

Lemaire V., Koehl M., LeMoal M. and Abrous D. N. (2000) Prenatal stress produces learning deficits associated with an inhibition of neurogenesis in the hippocampus. *Proc. Natl Acad. Sci. USA* **97**, 11032–11037.

Leuner B., Gould E. and Shors T. J. (2006) Is there a link between adult neurogenesis and learning? *Hippocampus* **16**, 216–224.

Lin Y., Bloodgood B. L., Hauser J. L., Lapan A. D., Koon A. C., Kim T. K., Hu L. S., Malik A. N. and Greenberg M. E. (2008) Activity-dependent regulation of inhibitory synapse development by Npas4. *Nature* **455**, 1198–1204.

Liu Y. W., Curtis M. A., Gibbons H. M., Mee E. W., Bergin P. S., Teoh H. H., Connor B., Dragunow M. and Faull R. L. (2008) Double-cortin expression in the normal and epileptic adult human brain. *Eur. J. Neurosci.* **28**, 2254–2265.

Lucassen P. J., Meerlo P., Naylor A. S., van Dam A. M., Dayer A. G., Fuchs E., Oomen C. A. and Czéh B. (2010) Regulation of adult neurogenesis by stress, sleep disruption, exercise and inflammation: implications for depression and antidepressant action. *Eur. Neuropsychopharmacol.* **20**, 1–17.

Magariños A. M. and McEwen B. S. (1995) Stress-induced atrophy of apical dendrites of hippocampal CA3c neurons: involvement of glucocorticoid secretion and excitatory amino acid receptors. *Neuroscience* **69**, 89–98.

Malberg J. E. and Duman R. S. (2003) Cell proliferation in adult hippocampus is decreased by inescapable stress: reversal by fluoxetine treatment. *Neuropsychopharmacology* **28**, 1562–1571.

Mirescu C. and Gould E. (2006) Stress and adult neurogenesis. *Hippocampus* **16**, 233–238.

Mirescu C., Peters J. D. and Gould E. (2004) Early life experience alters response of adult neurogenesis to stress. *Nat. Neurosci.* **7**, 841–846.

Mirescu C., Peters J. D., Noiman L. and Gould E. (2006) Sleep deprivation inhibits adult neurogenesis in the hippocampus by elevating glucocorticoids. *Proc. Natl Acad. Sci. USA* **103**, 19170–19175.

Montaron M. F., Drapeau E., Dupret D., Kitchener P., Aurousseau C., Le Moal M., Piazza P. V. and Abrous D. N. (2006) Lifelong corticosterone level determines age-related decline in neurogenesis and memory. *Neurobiol. Aging* **27**, 645–654.

Moser M., Knoth R., Bode C. and Patterson C. (2004) LE-PAS, a novel Arnt-dependent HLH-PAS protein, is expressed in limbic tissues and transactivates the CNS midline enhancer element. *Brain Res. Mol. Brain Res.* **128**, 141–149.

Nagai T., Yamada K., Kim H. C., Kim Y. S., Noda Y., Imura A., Nabeshima Y. and Nabeshima T. (2003) Cognition impairment in the genetic model of aging klotho gene mutant mice: a role of oxidative stress. *FASEB J.* **17**, 50–52.

Nagata K., Nakashima-Kamimura N., Mikami T., Ohsawa I. and Ohta S. (2009) Consumption of molecular hydrogen prevents the stress-induced impairments in hippocampus-dependent learning tasks during chronic physical restraint in mice. *Neuropsychopharmacology* **34**, 501–508.

Ooe N., Saito K., Mikami N., Nakatuka I. and Kaneko H. (2004) Identification of a novel basic helix-loop-helix-PAS factor, NXF, reveals a Sim2 competitive, positive role in dendritic-cytoskeleton modulator Drebrin gene expression. *Mol. Cell. Biol.* **24**(2), 608–616.

Ooe N., Motonaga K., Kobayashi K., Saito K. and Kaneko H. (2009) Functional characterization of basic helix-loop-helix-PAS type transcription factor NXF in vivo: putative involvement in an "on demand" neuroprotection system. *J. Biol. Chem.* **284**(2), 1057–1063.

Paxinos G. and Franklin K. B. J. (2004) *The Mouse Brain in Stereotaxic Coordinates*. Academic Press, San Diego.

Pham K., Nacher J., Hof P. R. and McEwen B. S. (2003) Repeated restraint stress suppresses neurogenesis and induces biphasic PSA-NCAM expression in the adult rat dentate gyrus. *Eur. J. Neurosci.* **17**, 879–886.

Phillips R. G. and LeDoux J. E. (1992) Differential contribution of amygdala and hippocampus to cued and contextual fear conditioning. *Behav. Neurosci.* **106**, 274–285.

Rakic P. (2002) Adult neurogenesis in mammals: an identity crisis. *J. Neurosci.* **22**, 614–618.

Reif A., Fritzen S., Finger M., Strobel A., Lauer M., Schmitt A. and Lesch K. P. (2006) Neural stem cell proliferation is decreased in schizophrenia, but not in depression. *Mol. Psychiatry* **11**, 514–522.

Reilly J. F., Games D., Rydel R. E., Freedman S., Schenk D., Young W. G., Morrison J. H. and Bloom F. E. (2003) Amyloid deposition in the hippocampus and entorhinal cortex: quantitative analysis of a transgenic mouse model. *Proc. Natl Acad. Sci. USA* **100**, 4837–4842.

Romanski L. M. and LeDoux J. E. (1992) Equipotentiality of thalamo-amygdala and thalamo-cortico-amygdala circuits in auditory fear conditioning. *J. Neurosci.* **12**, 4501–4509.

Sairanen M., Lucas G., Ernfors P., Castrén M. and Castrén E. (2005) Brain-derived neurotrophic factor and antidepressant drugs have different but coordinated effects on neuronal turnover, proliferation, and survival in the adult dentate gyrus. *J. Neurosci.* **25**, 1089–1094.

Scharfman H., Goodman J., Macleod A., Phani S., Antonelli C. and Croll S. (2005) Increased neurogenesis and the ectopic granule cells after intrahippocampal BDNF infusion in adult rats. *Exp. Neurol.* **192**, 348–356.

Segi-Nishida E., Warner-Schmidt J. L. and Duman R. S. (2008) Electroconvulsive seizure and VEGF increase the proliferation of neural stem-like cells in rat hippocampus. *Proc. Natl Acad. Sci. USA* **105**, 11352–11357.

Shors T. J., Miesegaes G., Beylin A., Zhao M., Rydel T. and Gould E. (2001) Neurogenesis in the adult is involved in the formation of trace memories. *Nature* **410**, 372–376.

Takuma K., Hoshina Y., Arai S. *et al.* (2007) Ginkgo biloba extract EGb 761 attenuates hippocampal neuronal loss and cognitive dysfunction resulting from chronic restraint stress in ovariectomized rats. *Neuroscience* **149**, 256–262.

Tamaki K., Yamada K., Nakamichi N., Taniura H. and Yoneda Y. (2008) Transient suppression of progenitor cell proliferation through NMDA receptors in hippocampal dentate gyrus of mice with traumatic stress experience. *J. Neurochem.* **105**, 1642–1655.

Tanapat P., Hastings N. B., Rydel T. A., Galea L. A. and Gould E. (2001) Exposure to fox odor inhibits cell proliferation in the hippocampus of adult rats via an adrenal hormone-dependent mechanism. *J. Comp. Neurol.* **437**, 496–504.

Tashiro A., Sandler V. M., Toni N., Zhao C. and Gage F. H. (2006) NMDA-receptor-mediated, cell-specific integration of new neurons in adult dentate gyrus. *Nature* **442**, 929–933.

Toni N., Laplagne D. A., Zhao C., Lombardi G., Ribak C. E., Gage F. H. and Schinder A. F. (2008) Neurons born in the adult dentate gyrus form frunctional synapses with target cells. *Nat. Neurosci.* **11**, 901–907.

Vaidya V. A., Terwilliger R. M. and Duman R. S. (1999) Role of 5-HT2A receptors in the stress-induced down-regulation of brain-derived neurotrophic factor expression in rat hippocampus. *Neurosci. Lett.* **262**, 1–4.

Veena J., Srikumar B. N., Mahati K., Bhagya V., Raju T. R. and Shankaranarayana Rao B. S. (2009) Enriched environment restores hippocampal cell proliferation and ameliorates cognitive deficits in chronically stressed rats. *J. Neurosci. Res.* **87**, 831–843.

Watanabe Y., Gould E. and McEwen B. S. (1992) Stress induces atrophy of apical dendrites of hippocampal CA3 pyramidal neurons. *Brain Res.* **588**, 341–345.

Westenbroek C., Den Boer J. A., Veenhuis M. and Ter Horst G. J. (2004) Chronic stress and social housing differentially affect neurogenesis in male and female rats. *Brain Res. Bull.* **64**, 303–308.

Winocur G., Wojtowicz J. M., Sekeres M., Snyder J. S. and Wang S. (2006) Inhibition of neurogenesis interferes with hippocampus-dependent memory function. *Hippocampus* **16**, 296–304.

Xu H., Chen Z., He J., Haimanot S., Li X., Dyck L. and Li X. M. (2006) Synergetic effects of quetiapine and venlafaxine in preventing the chronic restraint stress-induced decrease in cell proliferation and BDNF expression in rat hippocampus. *Hippocampus* **16**, 551–559.

Yap J. J., Takase L. F., Kochman L. J., Fornal C. A., Miczek K. A. and Jacobs B. L. (2006) Repeated brief social defeat episodes in mice: effects on cell proliferation in the dentate gyrus. *Behav. Brain Res.* **172**, 344–350.

Yoneyama M., Fukui M., Nakamichi N., Kitayama T., Taniura H. and Yoneda Y. (2007) Activation of GABAA receptors facilitates astroglial differentiation induced by ciliary neurotrophic factor in neural progenitors isolated from fetal rat brain. *J. Neurochem.* **100**, 1667–1679.

Yoneyama M., Seko K., Kawada K., Gotoh Y., Nagashima R., Sugiyama C., Kuramoto N. and Ogita K. (2009) High susceptibility of cortical neural progenitor cells trimetyltin toxicity: involvement of caspases and calpain in cell death. *Neurochem. Int.* **55**, 257–264.

Zhang C. L., Zou Y., He W., Gage F. H. and Evans R. M. (2008) A role for adult TLX-positive neural stem cells in learning and behaviour. *Nature* **451**, 1004–1007.

J Pharmacol Sci 113, 404 – 408 (2010)

Journal of Pharmacological Sciences

Short Communication

Parishin C Attenuates Phencyclidine-Induced Schizophrenia-Like Psychosis in Mice: Involvements of 5-HT$_{1A}$ Receptor

Eun-Joo Shin[1,†], Wan Kyunn Whang[2,†], Sungun Kim[2], Jae-Hyung Bach[1], Jin-Man Kim[1], Xuan-Khanh Thi Nguyen[1], Thuy-Ty Lan Nguyen[1], Bae Dong Jung[3], Kiyofumi Yamada[4], Toshitaka Nabeshima[5], and Hyoung-Chun Kim[1,*]

[1]*Neuropsychopharmacology and Toxicology Program, College of Pharmacy,* [3]*School of Veterinary Medicine, Kangwon National University, Chunchon 200-701, Korea*

[2]*Phamaceutical Resources Botany, College of Pharmacy, Chung-Ang University, Seoul 156-756, Korea*

[4]*Department of Neuropsychopharmacology and Hospital Pharmacy, Nagoya University Graduate School of Medicine, Nagoya 466-8560, Japan*

[5]*Department of Chemical Pharmacology, Graduate School of Pharmaceutical Sciences, Meijo University, Nagoya 468-8503, Japan*

Received February 4, 2010; Accepted June 1, 2010

Abstract. Parishin C, a major component of *Gastrodia elata* BLUME (GE), was purified from GE. Because GE modulates the serotonergic system and the 5-HT$_{1A}$ receptor is an important therapeutic target of schizophrenia, we examined whether parishin C affects phencyclidine-induced abnormal behaviors in mice. Phencyclidine-induced abnormal behaviors were significantly ameliorated by parishin C. These effects were reversed by WAY 100635, a 5-HT$_{1A}$–receptor antagonist. Consistently, parishin C showed high affinity at 5-HT$_{1A}$ receptor as well as a 5-HT$_{1A}$–agonist activity in a 8-OH-DPAT–stimulated [^{35}S]GTP-γS binding assay. Our results suggest that the antipsychotic effects of parishin C require activation of 5-HT$_{1A}$ receptors.

Keywords: parishin C, phencyclidine, 5-HT$_{1A}$ receptor

Gastrodia elata BLUME (GE) is a well-known herbal agent that has long been used to treat headache, paralysis, epileptic convulsion, and other neurological disorders in traditional oriental medicine. Recently, it was demonstrated that GE significantly decreased immobility duration in a forced-swimming test in rats, primarily by modulating the serotonergic system (1).

It was suggested that serotonin 5-HT$_{1A}$ receptors play a role in the pathophysiology of psychiatric diseases, including schizophrenia, and that 5-HT$_{1A}$ receptors might be an important target for emotion and cognition (2).

Phencyclidine [1-(1-phenylcyclohexyl)piperidine hydrochloride (PCP)] a non-competitive *N*-methyl-D-aspartate (NMDA) antagonist, has been shown to a induce schizophrenia-like psychosis, with positive symptoms, negative symptoms, and cognitive deficits in humans, which persist for several weeks after withdrawal from chronic PCP use (3).

To understand the pathophysiology of schizophrenia, an animal model of schizophrenia was established using PCP (3). Nabeshima and colleagues previously demonstrated that repeated treatment with PCP induced several behavioral abnormalities such as increased immobility in a forced swimming test, social deficits on a social interaction test, impairment of latent learning in a water finding test, and associative learning impairment in cue and contextual fear conditional tests in mice (3). Thus, PCP-treated mice might be a useful animal model of schizophrenia.

In the present study, we purified parishin C from GE. We examined whether parishin C affects PCP-induced changes in immobility, social interaction, and cognitive function in mice. Simultaneously, we evaluated whether the 5-HT$_{1A}$ receptor is involved in parishin C–mediated pharmacological actions against PCP insults.

All animals were treated in accordance with the NIH Guide for the Care and Use of Laboratory Animals (NIH

†These authors contributed equally to this work.
*Corresponding author. kimhc@kangwon.ac.kr
Published online in J-STAGE on July 13, 2010 (in advance)
doi: 10.1254/jphs.10040SC

Publication No. 85-23, 1985; www.dels.nas.edu/ila). This study was performed in accordance with the Institute for Laboratory Animal Research (ILAR) guidelines for the care and use of laboratory animals.

Male C57BL/6J mice or male ICR mice (Bio Genomic Inc., Gyeonggi-Do, South Korea), weighing 25 ± 3 g, were maintained on a 12:12 h light:dark cycle and fed ad libitum. Male ICR mice were only used as the "target" in the social interaction test, with no drug treatment.

N-[2-[4-(2-Methoxyphenyl)-1-piperazinyl]ethyl-*N*-(2-pyridinyl)cyclohexane carboxamide trihydrochloride (WAY 100635; Sigma-Aldrich, St. Louis, MO, USA), PCP hydrochloride (Tocris Bioscience, Ellisville, MO, USA), and (+)-8-hydroxy-2-(di-*n*-propylamino)tetralin (8-OH-DPAT, Sigma-Aldrich) were dissolved in 0.9% sterile saline. 1,3-Bis[4-*β*-D-glucopyranosyloxy)benzyl] citrate (Parishin C, Fig. 1A) was purified according to Lin et al. (4) and was dissolved in distilled water. All solutions were prepared immediately before use. Mice received PCP (10 mg·kg^{-1}·day^{-1}, s.c.) for consecutive 14 days. Parishin C (25, 50, or 100 mg·kg^{-1}·day^{-1}, i.p.) or 8-OH-DPAT (0.05 mg·kg^{-1}·day^{-1}, i.p.) was administered throughout the experimental period (26 days). Mice received WAY 100635 (0.5 mg·kg^{-1}·day^{-1}, i.p.) during the PCP withdrawal period. Novel object recognition, forced swimming, and social interaction tests were performed 7 days after withdrawal from PCP. As reflected by the efficacy of parishin C (or GE), pre-treatment is more effective than post-treatment in response to PCP in our pilot study (5). Thus, we used the experimental schedule of our pilot study in our current study (5). Experimental schedules are shown in Fig. 1B.

The novel object recognition, forced swimming, and social interaction tests were performed as described previously (1, 6, 7). An automated video-tracking system (Noldus Information Technology, Wageningen, Netherlands) was used to record and analyze the movements of mice in all three tests. Binding study to 5-HT$_{1A}$ receptors was performed using rat hippocampal membrane according to the procedure described by Hoyer et al. (8). The

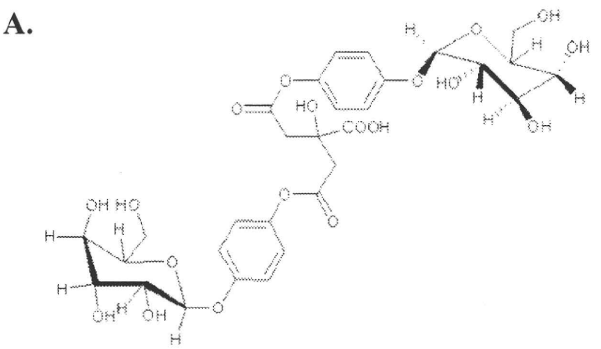

Fig. 1. Chemical structure of parishin C (A) and experimental schedules (B). 8-OH-DPAT was used as a reference drug. Mice were treated with phencyclidine (PCP) (10 mg·kg^{-1}·day^{-1}, s.c.) for 14 consecutive days. After a 7- or 8-day withdrawal period, the novel object recognition, forced swimming, and social interaction tests were performed using independent sets of mice; each set of mice was used for one of the three behavioral tests (&). Treatment with parishin C (25, 50, or 100 mg·kg^{-1}·day^{-1}, i.p.) or 8-OH-DPAT (0.05 mg·kg^{-1}·day^{-1}, i.p.) was started from 4 days before the first PCP injection and continued throughout the experimental period. WAY 100635 (0.5 mg·kg^{-1}·day^{-1}, i.p.) was administered during the PCP withdrawal period. Parishin C was injected 90 min prior to PCP or WAY 100635, and WAY 100635 was injected 30 min prior to the behavior test.

inhibition constants (*Ki*) were calculated from the Cheng and Prusoff equation (9). For the [^{35}S]GTPγS binding assay, membranes were prepared from rat hippocampus according to the method described by Alper and Nelson (10). The agonist activity of increasing concentrations of parishin C was determined by stimulation of [^{35}S]GTPγS binding.

Statistical analyses were performed using one-way analysis of variance (ANOVA). A *post-hoc* Fisher's PLSD test or a Student–Newman-Keuls test was then applied. A P value < 0.05 was deemed to indicate statistical significance.

Repeated treatment with PCP (10 mg·kg^{-1}·day^{-1}, s.c.) resulted in significant increases in immobility time in the forced swimming test, while PCP resulted in significant decreases in the interaction time in the social interaction test and exploration rate for a novel object in the novel object recognition test. Parishin C treatment (50 or 100 mg·kg^{-1}, i.p.) significantly attenuated PCP-induced increase in immobility time, sociability deficit, and impaired visual recognition memory in a dose-dependent manner. The effects of parishin C (100 mg·kg^{-1}, i.p.) in all behaviors were comparable to those of 8-OH-DPAT (0.05 mg·kg^{-1}, i.p.), a 5-HT$_{1A}$–receptor agonist. Consistently, WAY 100635 (0.5 mg·kg^{-1}, i.p.), a 5-HT$_{1A}$–receptor antagonist, significantly inhibited parishin C (100 mg·kg^{-1}, i.p.)–mediated pharmacological actions in response to PCP (Fig. 2).

The apparent affinity (*Ki*) of parishin C and the reference compound 8-OH-DPAT labeled by [^{3}H]-8-OH-DPAT in rat hippocampal membrane were determined. As shown in Table 1, parishin C exhibited high affinity at 5-HT$_{1A}$ receptors (*Ki* = 1.54 nM), which is comparable to 8-OH-DPAT (*Ki* = 1.21 nM). For agonist activity, the effect of parishin C was compared with the selective 5-HT$_{1A}$–receptor agonist *R*(+)-5-OH-DPAT for stimulation of [^{35}S]GTPγS binding. Parishin C produced a significant stimulation (% increase = 78.4) in a concentration-dependent manner (EC_{50} = 34 nM); this is near the *R*(+)-8-OH-DPAT level (% increase = 93.6), suggesting that parishin C is a 5-HT$_{1A}$–receptor full agonist. Thus, it is possible that parishin C attenuates PCP-induced changes in immobility time, social interaction, and cognitive function, at least in part, via activation of 5-HT$_{1A}$ receptors.

A recent finding has suggested that repeated PCP treatment significantly decreases the density of 5-HT$_{1A}$ receptors in the mouse brain (11). 5-HT$_{1A}$–agonist properties are thought to improve negative symptoms and cognitive deficits by stimulating the release of dopamine in the prefrontal cortex (12). Atypical antipsychotic drugs, such as clozapine, zipraidone, aripiprazole, and quetiapine, are all 5-HT$_{1A}$–receptor (partial) agonists, which may be relevant for their actions in treating schizophrenia (13). While current antipsychotic treatments are effective against positive symptoms, they have significant side effects and have little effect on negative

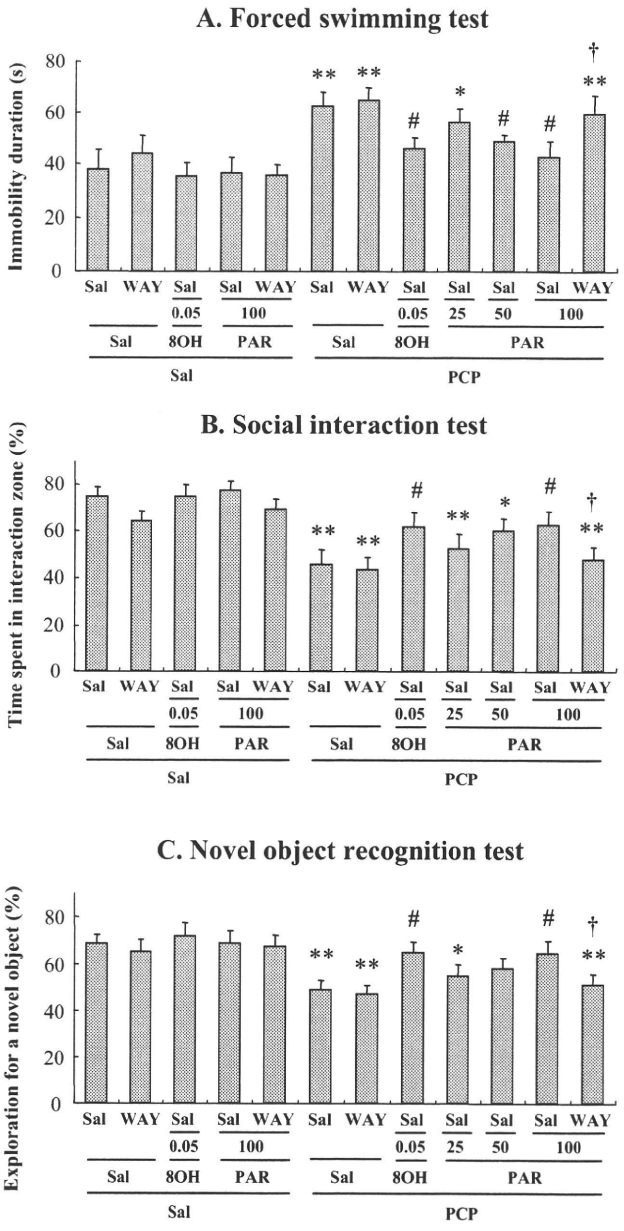

Fig. 2. Effect of WAY 100635 on the parishin C–mediated pharmacological actions in response to phencyclidine (PCP)-induced changes in the immobility time (A), social interaction time (B), and recognition memory (C). Sal = saline, PAR 25 = parishin C (25 mg·kg^{-1}, i.p.), PAR 50 = parishin C (50 mg·kg^{-1}, i.p.), PAR 100 = parishin C (100 mg·kg^{-1}, i.p.), 8OH = 8-OH-DPAT (0.5 mg·kg^{-1}, i.p.), WAY = WAY 100635 (0.5 mg·kg^{-1}, i.p.). Each value is the mean ± S.E.M. of 12 mice. *P < 0.05, **P < 0.01 vs. Saline + Saline + Saline; $^{\#}P$ < 0.05 vs. Saline + Saline + PCP; $^{\dagger}P$ < 0.05 vs. Saline + PAR 100 + PCP (One-way ANOVA followed by Fisher's PLSD test).

Table 1. Affinity for 5-HT_{1A} receptors and agonist properties of [^{35}S]GTPγS binding in isolated rat hippocampal membranes

Compound	*Ki* (nM)	Basal fmol GTPγS (bound/mg protein)	Maximal fmol GTPγS (bound/mg protein)	Increase (%)
R(+)-8-OH-DPAT	1.21 ± 0.02	14.1 ± 0.9	27.3 ± 1.4	93.6**
Parishin C	1.54 ± 0.04	13.9 ± 1.2	24.8 ± 2.5	78.4**

Compounds were tested at concentrations from 10^{-10} to 10^{-5} M. Each value is the mean ± S.E.M. of three separate experiments. Significant increase, $^{**}P < 0.01$ (One-way ANOVA followed by Student–Newman-Keuls test).

or cognitive symptoms (14).

Nagai et al. (7) have indicated that potential antipsychotic effects on PCP require combined modulation of 5-HT_{1A} and dopamine receptors. Interestingly, the GE-mediated anti-depressant effects are exerted, at least in part, by dopaminergic modulation in the rat brain (1); however, the interaction between 5-HT_{1A} and specific dopamine receptors in our experimental condition remains to be determined.

Our results are in line with our earlier findings that repeated treatment with PCP showed significant increases in immobility time and significant decreases in social interaction and recognition memory in mice (3). Prolonged exposure to parishin C significantly blocked PCP-induced behavioral effects, in a dose-related manner. The protective effects of parishin C in response to PCP were comparable to those of the 5-HT_{1A}–receptor agonist 8-OH-DPAT (0.05 mg·kg^{-1}, i.p.). Furthermore, our results suggest that parishin C is a 5-HT_{1A} full agonist with high affinity at 5-HT_{1A} receptors. Consistently, the 5-HT_{1A}–receptor antagonist WAY 100635 significantly counteracted parishin C–mediated pharmacological effects in response to PCP. We propose that the 5-HT_{1A} full agonistic character of parishin C may be important in its antipsychotic effects in response to PCP. Alternatively, we cannot rule out the possibility that parishin C might act as a 5-HT receptor–transporter inhibitor. However, the effective doses, 100 and 0.05 mg·kg^{-1} for parishin C and 8-OH-DPAT, respectively, are quite different. It may be due to pharmacokinetic differences between both compounds or parishin C might exert its effect through mechanisms other than 5-HT_{1A}–receptor activation.

Similar to parishin C, various 5HT_{1A}–receptor agonists, such as buspirone, 8-OH-DPAT, and ipsapirione, have been shown to enhance social interaction (15). Furthermore, various preclinical data strengthen the notion that targeting the 5-HT_{1A}–receptor system should result in beneficial effects on dysfunctional social behavior, possibly not only in schizophrenic patients but also in the population suffering from social withdrawal of other etiologies.

Interestingly, Hagiwara et al. (11) demonstrated that the hippocampal density of 5-HT_{1A} receptor is much higher than the frontal cortical density of 5-HT receptor in mice and that repeated treatment with PCP did not significantly alter the frontal cortical density of 5-HT, but did change the hippocampal density of 5-HT receptors, and that perospirone, a 5-HT_{1A}–receptor agonist, ameliorated PCP-induced cognitive deficits, as measured by a novel object recognition test (NORT). Thus, the cognitive enhancing effect of parishin C or 8-OH-DPAT may be similar to that of perospirone.

Combined, our results suggest that 5-HT_{1A} receptor–agonistic properties of parishin C offer potential therapeutic advantages in response to PCP-induced schizophrenia-like psychosis.

Acknowledgments

This study was supported by a grant from the Brain Research Center from the 21st Century Frontier Research Program funded by the Ministry of Science and Technology, Republic of Korea. This work was, in part, supported by grants from the Ministry of Health, Labour and Welfare, Japan (MHLW): Research on Risk of Chemical Substances and the Ministry of Education, Culture, Sports, Science and Technology, Japan (MEXT): Academic Frontier Project. Jin-Man Kim and Jae-Hyung Bach were supported by the BK 21 program. Equipment at the Institute of Pharmaceutical Science (Kangwon National University) was used for this study.

References

1 Chen PJ, Hsieh CL, Su KP, Hou YC, Chiang HM, Sheen LY. Rhizomes of *Gastrodia elata* B_L possess antidepressant-like effect via monoamine modulation in subchronic animal model. Am J Chin Med. 2009;37:1113–1124.

2 Meltzer HY. The role of serotonin in antipsychotic drug action. Neuropsychopharmacology. 1999;21:106S–115S.

3 Mouri A, Noda Y, Enomoto T, Nabeshima T. Phencyclidine animal models of schizophrenia: approaches from abnormality of glutamatergic neurotransmission and neurodevelopment. Neurochem Int. 2007;51:173–184.

4 Lin JH, Liu YC, Hau JP, Wen KC. Parishins B and C from rhizomes of gastrodia elata. Phytochemistry. 1996;42:549–551.

5 Shin EJ, Kim JM, Jin CH, Bach JH, Kim HC. Gastrodia elata attenuates phencyclidine-induced schizophrenia-like psychosis in mice. In: Recent frontiers & advances in drug addiction, Proceed-

ings of the 2nd International Drug Abuse Research Society & International Society for Neurochemistry Satellite Meeting in association with Korean Society for Drug Abuse Research; 2009 Aug 17-21; Seoul, Korea: P 125.

6 Krishnan V, Han MH, Mazei-Robison M, Iñiguez SD, Ables JL, Vialou V, et al. AKT signaling within the ventral tegmental area regulates cellular and behavioral responses to stressful stimuli. Biol Psychiatry. 2008;64:691–700.

7 Nagai T, Murai R, Matsui K, Kamei H, Noda Y, Furukawa H, et al. Aripirazole ameliorates phencyclidine-induced impairment of recognition memory through dopamine D_1 and serotonin 5-HT_{1A} receptors. Psychopharmacology. 2009;202:315–328.

8 Hoyer D, Engel G, Kalhman HO. Molecular pharmacology of 5-HT_1 and 5-HT_2 recognition sites in rat and pig brain membranes radioligand binding sites with [^{3}H]-ketanserin. Eur J Pharmacol. 1985;118:13–23.

9 Cheng YC, Prossof WH. Relationship between the inhibition constant (Ki) and the concentration of inhibitor which causes 50% inhibition (IC_{50}) of a enzymatic reaction. Biochem Pharmacol. 1973;22:3099–3108.

10 Alper RH, Nelson DL. Characterization of 5-HT_{1A} receptor-mediated [^{35}S]GTPγS binding in rat hippocampal membranes. Eur J Pharmacol. 1998;343:303–312.

11 Hagiwara H, Fusita Y, Ishima T, Kunitachi S, Shirayama Y, Iyo M, et al. Phencyclidine-induced cognitive deficits in mice are improved by subsequent subchronic administration of the antipsychotic drug perospirone: role of serotonin 5-HT_{1A} receptors. Eur Neuropsychopharmacol. 2008;18:448–454.

12 Ichikawa J, Meltzer HY. Relationship between dopaminergic and serotonergic neuronal activity in the frontal cortex and the action of typical and atypical antipsychotic drugs. Eur Arch Psychiatry Clin Neurosci. 1999;249:90–98.

13 Rollema H, Lu Y, Schmidt AW, Sprouse JS, Zorn SH. 5-TH_{1A} receptor activation contributes to ziprasidone-induced dopamine release in the rat prefrontal cortex. Biol Psychiatry. 2000;48: 229–237.

14 Green MF, Kern RS, Braff DL, Mintz J. Neurocognitive deficits and functional outcome in schizophrenia: are we measuring the "right stuff"? Schizophr Bull. 2000;26:119–136.

15 File SE, Seth P. A review of 25 years of the social interaction test. Eur J Pharmacol. 2003;463:35–53.

0022-3565/08/3271-137–147$20.00
THE JOURNAL OF PHARMACOLOGY AND EXPERIMENTAL THERAPEUTICS
Copyright © 2008 by The American Society for Pharmacology and Experimental Therapeutics
JPET 327:137–147, 2008

Vol. 327, No. 1
141309/3384925
Printed in U.S.A.

The Extensive Nitration of Neurofilament Light Chain in the Hippocampus Is Associated with the Cognitive Impairment Induced by Amyloid β in Mice

Tursun Alkam, Atsumi Nitta, Hiroyuki Mizoguchi, Akio Itoh, Rina Murai, Taku Nagai, Kiyofumi Yamada, and Toshitaka Nabeshima

Department of Neuropsychopharmacology and Hospital Pharmacy, Nagoya University Graduate School of Medicine, Nagoya, Japan (T.A., A.N., H.M., A.I., R.M., T.Nag., K.Y., T.Nab.); Department of Basic Medicine, College of Traditional Uighur Medicine, Hotan, China (T.A.); and Department of Chemical Pharmacology, Graduate School of Pharmaceutical Science, Meijo University, Nagoya, Japan (T.Nab.)

Received May 19, 2008; accepted July 9, 2008

ABSTRACT

Tyrosine nitration of proteins at an extensive level is widely associated with the cognitive pathology induced by amyloid β peptide (Aβ). However, the precise identity and explicit consequences of protein nitration have scarcely been addressed. In this study, we examined the detectable nitration of proteins in the hippocampus of mice with cognitive impairment (day 5) induced by the i.c.v. injection of $A\beta_{25-35}$ (day 0). The intensity of the nitration of proteins was inversely associated with the level of recognition memory in mice. The detectable tyrosine nitrations were revealed in proteins with a single size of approximately 70 kDa. The specific nitrated proteins at this size were identified using the liquid chromatography/mass spectrometry/mass spectrometry analysis and immunodetection methods. Intense nitration of the neurofilament light chain (NFL) was observed. The increased nitration of NFL was associated with its serine hyperphosphorylation and weak interaction with the nuclear distribution element-like, a protein essential for the stable assembly of neurofilaments. No changes in cell numbers in the hippocampus were found (day 5) in mice that received $A\beta_{25-35}$ injections. These findings suggested that extensive nitration of NFL is associated with the Aβ-induced impairment of recognition memory in mice.

Increased nitration of proteins, a surrogate marker of widespread oxidative damage in brains affected by the amyloid β peptide (Aβ), is evidently correlated with the severity of cognitive dysfunction in humans as well as animals (Smith et al., 1997; Lim at al., 2001; Perry et al., 2002; Kim et al., 2003; Andersen, 2004; Bastianetto and Quirion, 2004; Walsh and Selkoe, 2004).

We have previously reported the contribution of tyrosine nitration to Aβ-induced, oxidative damage-mediated cognitive dysfunction in mice (Alkam et al., 2007, 2008). A mouse monoclonal anti-nitrotyrosine antibody in Western blot analysis identified the tyrosine-nitrated hippocampal proteins at approximately 70 kDa as a single band with which the severity of cognitive impairments in mice was well associated (Alkam et al., 2007). In this study, we aimed to identify the nitrated proteins in the single band for the specification of the contribution of the extensive nitration of tyrosine to the cognitive impairment. To produce strong and stable nitrative damage, we applied $A\beta_{25-35}$, a toxic Aβ fragment that is detected in the human brain (Pike et al., 1995; Kubo et al., 2002). The tyrosine-nitrated proteins were examined by using liquid chromatography/mass spectrometry/mass spec-

This work was supported, in part, by the following: Japan-China Sasakawa Medical fellowship (to T.A.); Uehara Memorial Foundation fellowship for Foreign Researchers in Japan (to T.A.); grant-in-aid for the 21st Century Center of Excellence Program "Integrated Molecular Medicine for Neuronal and Neoplastic Disorders" and "Academic Frontier Project for Private Universities (2007–2011)" from the Ministry of Education, Culture, Sports, Science and Technology of Japan; Comprehensive Research on Aging and Health from the Ministry of Health, Labor and Welfare of Japan; Japan-Canada Joint Health Research Program and Japan-France Joint Health Research Program (Joint Project from Japan Society for the Promotion of Science); and International Research Project Supported by the Meijo Asian Research Center.

Article, publication date, and citation information can be found at http://jpet.aspetjournals.org.

doi:10.1124/jpet.108.141309.

ABBREVIATIONS: Aβ, amyloid β peptide; LC-MS/MS, liquid chromatography/mass spectrometry/mass spectrometry; NFL, neurofilament light chain; NUDEL, nuclear distribution element-like; NF, neurofilament; $ONOO^-$, peroxynitrite; UA, uric acid; RIPA, radioimmunoprecipitation assay; PBS, phosphate-buffered saline; PAGE, polyacrylamide gel electrophoresis; PVDF, polyvinylidene difluoride; HSP70, heat shock protein 70; DRP-2, dihydropyrimidinase-like 2; GAPDH, glyceraldehyde 3-phosphate dehydrogenase; SD, sodium dithionite; CBB, Coomassie Brilliant Blue; AD, Alzheimer's disease.

trometry (LC-MS/MS) and immunodetection. Intense nitration of the neurofilament light chain (NFL) was observed. The intensive nitration was associated with serine hyperphosphorylation and reduced interaction of NFL with nuclear distribution element-like (NUDEL), a protein essential for the stable assembly of neurofilaments (NFs). The results provided further support for the conception that extensive nitration of tyrosine in proteins underlies one of the key mechanisms contributing to the cognitive pathology induced by Aβ.

Materials and Methods

Animals. Male ICR mice (Nihon SLC Co., Shizuoka, Japan) were used. The animals were housed in a controlled environment (23 ± 1°C, 50 ± 5% humidity) and allowed access to food and water ad libitum. The room lights were kept on between 8:00 AM and 8:00 PM. All experiments were performed in accordance with the Guidelines for Animal Experiments of Nagoya University Graduate School of Medicine. The procedures involving animals and their care conformed to the *Guidelines for Proper Conduct of Animal Experiments* (Science Council of Japan, 2006).

Treatment and Experimental Design. $A\beta_{25-35}$ (Bachem, Bubendorf, Switzerland) was dissolved in sterile double-distilled water to a stock concentration of 1 mg/ml and stored at −20°C before use. The dissolved $A\beta_{25-35}$ was incubated for aggregation at 37°C for 4 days. The distilled water was incubated at the same conditions and used as the vehicle. $A\beta_{1-40}$ (Bachem) was dissolved to a stock concentration of 1.0 mg/ml in 35% acetonitrile/0.1% trifluoroacetic acid and stored at −20°C before use. The solution of peroxynitrite ($ONOO^-$; 144 mM) (Millipore, Billerica, MA) was stored at −80°C before use. Incubated $A\beta_{25-35}$ (3 μg/3 μl), incubated distilled water (3 μl), $A\beta_{1-40}$ (5 μg/5 μl), and $ONOO^-$ (144 mM/1 μl) were administered by i.c.v. injection as described previously (Maurice et al., 1996; Alkam et al., 2007, 2008). In brief, a microsyringe with a 28-gauge stainless steel needle 3.0-mm long was used for all experiments. Mice were anesthetized lightly with ether, and the needle was inserted unilaterally 1 mm to the right of the midline point equidistant from each eye, at an equal distance between the eyes and the ears and perpendicular to the plane of the skull. A single shot of the indicated volume of agents was delivered gradually within 3 s. Mice exhibited normal behavior within 1 min after the injection. The injection placement or needle track was visible and was verified at the time of dissection. Neither insertion of the needle nor the volume of injection had a significant influence on survival, behavioral responses, or cognitive functions. Uric acid (UA) (Wako Pure Chemicals, Osaka, Japan) was prepared as a suspension in saline. Immediately after the single injection of $A\beta_{25-35}$ or $A\beta_{1-40}$, mice were given UA (100 mg/kg i.p.) daily for 6 consecutive days. The schedule of administration of peptides and drugs as well as biochemical, histochemical, and behavioral investigations is shown in Fig. 1.

Novel Object Recognition Task. This task, based on the spontaneous tendency of rodents to explore a novel object more often than a familiar one, was performed on days 3 to 5 after the i.c.v. injection of $A\beta_{1-40}$, $A\beta_{25-35}$, or peroxynitrite (day 0) as described previously (Alkam et al., 2007). A plastic chamber (35 × 35 × 35 cm) was used in low light conditions during the light phase of the light/dark cycle. The general procedure consisted of three different phases: 1) a habituation phase, 2) an acquisition phase, and 3) a retention phase. On the 1st day (habituation phase), mice were individually subjected to a single familiarization session of 10 min, during which time they were introduced into the empty arena to become familiar with the apparatus. On the 2nd day (acquisition phase), the animals were subjected to a single 10-min session, during which time two floor-fixed objects (A and B) were placed in a symmetric position from the center of the arena, 15 cm from each other and 8 cm from the nearest wall. The two objects, made of the same wooden material with a similar color and smell, were different in shape but identical in size. Mice were allowed to explore the objects in the open field. A preference index for each mouse was expressed as a ratio of the amount of time spent exploring object A (TA × 100)/(TA + TB), where TA and TB are the time spent exploring object A and object B, respectively. On the 3rd day (retention phase), mice were allowed to explore the open field in the presence of two objects: the familiar object A and a novel object C in different shapes but in similar color and size (A and C). A recognition index, calculated for each mouse, was expressed as the ratio (TC × 100)/(TA + TC), where TA and TC are the time spent during the retention phase on object A and object C, respectively. The time spent exploring the object (nose pointing toward the object at a distance ≤ 1 cm) was recorded by hand.

Sample Preparation. Animals were decapitated, and the hippocampi were removed on an ice-cold glass plate and stored at −80°C. Hippocampal protein extracts were obtained by homogenization in diverse ice-cold lysis buffers that included the radioimmunoprecipitation assay (RIPA) buffer, phosphate-buffered saline (PBS) buffer, Triton X-100 buffer, and 6 M urea buffer. The RIPA lysis buffer contained 20 mM trizma hydrochloride, pH 7.6, 150 mM sodium chloride, 2 mM EDTA·2Na, 50 mM sodium fluoride, 1 mM sodium vanadate, 1% Nonidet P-40, 1% sodium deoxycholate, 0.1% SDS, 1 mg/ml pepstatin, 1 mg/ml aprotinin, and 1 mg/ml leupeptin. The PBS lysis buffer, pH 7.4, contained 135 mM sodium chloride, 3.2 mM disodium hydrogen phosphate 12-water, 1.3 mM potassium chloride, and 0.5 mM potassium dihydrogen phosphate. The Triton X-100 buffer contained 10 mM trizma hydrochloride at pH 7.5, 150 mM sodium chloride, 1 mM EDTA at pH 8.0, and 1% Triton X-100. The 6 M urea lysis buffer contained 10 mM trizma base at pH 8.1, 6 M urea, and 1 mM dithiothreitol. All of these lysis buffers, with the exception of the RIPA buffer, were supplemented with complete protease inhibitor cocktail tablets (Roche Applied Science, Mannheim, Germany). Homogenates were centrifuged at 13000*g* for 20 min to obtain the desired supernatant of the extracts. The centrifuged pellets were washed twice with the previous buffer before being solubilized. The washing procedure consisted of complete dispersion of the pellets by vortexing and incubation in ice for 30 min followed by centrifugation at 13000*g* for 20 min. The unassembled NFL and NUDEL proteins were obtained within the soluble proteins in Triton X-100 buffer (Nguyen et al., 2004), and the insoluble protein pellets that include the assembled NFL and NUDEL proteins were then solubilized in 6 M urea lysis buffer (Crow et al., 1997). The cytoplasmic water-soluble proteins were obtained in PBS lysis buffer (Aoyama and Kitajima, 1999), and the insoluble pellets were then solubilized in Triton X-100 buffer. The concentrations of PBS-soluble and urea-soluble proteins were determined with a Bio-Rad protein assay reagent kit (Bio-Rad, Hercules, CA). The concentrations of the Triton

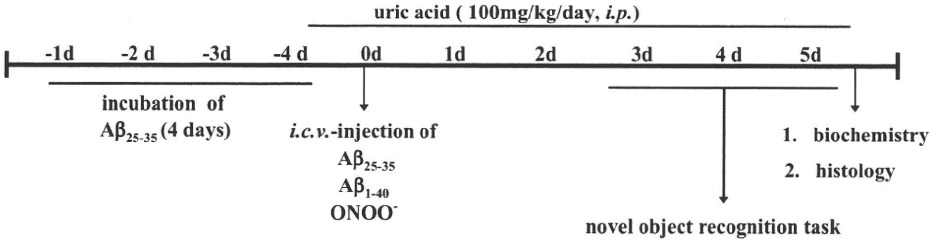

Fig. 1. The experimental design of the study.

X-100-soluble proteins were determined with a BCA protein assay reagent kit (Pierce, Rockford, IL).

Western Blot Analysis. Equal amounts (20 μg) of protein sample were resolved by a 4 to 20% gradient or 7% SDS-polyacrylamide gel electrophoresis (PAGE). The proteins were then transferred electrophoretically to a polyvinylidene difluoride (PVDF) membrane (Millipore). Membranes were incubated in 3% skim milk or 3% bovine serum albumin (for phosphor-protein) in phosphate-buffered saline containing 0.05% (v/v) Tween 20 for 2 h at room temperature. Anti-nitrotyrosine mouse monoclonal 1A6 antibody (catalog number 05-233; Millipore), anti-NFL mouse antibody (Sigma-Aldrich, St. Louis, MO), anti-heat shock protein 70 (HSP70) polyclonal antibody (Assay Designs, Ann Arbor, MI), anti-dihydropyrimidinase-like 2 (DRP-2) mouse antibody (IBL, Takasaki, Japan), anti-NUDEL rabbit antibody (Abcam Inc., Cambridge, MA), anti-phosphoserine rabbit antibody (Zymed Laboratories, South San Francisco, CA), anti-β-actin goat antibody (Santa Cruz Biotechnology Inc., Santa Crutz, CA), and anti-glyceraldehyde 3-phosphate dehydrogenase (GAPDH) mouse antibody (Imgenex, San Diego, CA) were used. To confirm the specificity of the detected single band of tyrosine-nitrated proteins, the reduction of nitrotyrosine to aminotyrosine was performed. In brief, the membrane was treated with 10 mM sodium dithionite (SD) in 50 mM pyridine-acetate buffer, pH 5.0, for 1 h at room temperature. After the reaction, the membrane was rinsed with distilled water and then equilibrated with washing buffer and blocked for 1 h at room temperature in blocking solution before standard procedures of Western blotting were followed. The absent band in the SD-treated membrane compared with the routine-treated control membrane was regarded to be a genuine for nitrated proteins. To confirm the specificity of the detected band for phosphoserine, the anti-phosphoserine inhibitor (the inhibitor) that contains phosphoserine was used to block the specific interaction of anti-phosphoserine primary antibodies with serine-phosphorylated proteins in the membrane. In brief, the anti-phosphoserine primary antibody and the inhibitor at a final concentration of 20 mM were mixed into a bovine serum albumin-containing blocking buffer and preincubated for 10 min for the ample binding of the antibodies with the phosphoserines (to cover up all of the specific anti-phosphoserine antibodies) before the application to the membrane. Incubation of the antibody-inhibitor mixture with the membrane was carried out for 1 h at room temperature. After the incubation, standard procedures were followed for blot washing and incubation with a secondary antibody. The absence of the bands in the membrane after the antibody-inhibitor treatment compared with the membrane subjected to routine treatment was regarded as genuine proof of serine phosphorylation. The intensity of each protein band on the film was analyzed with the Atto Densitograph 4.1 system (Atto, Tokyo, Japan) and was corrected with the corresponding β-actin or GAPDH level. The results were expressed as a percentage of that in the naive group.

Liquid Chromatography/Mass Spectrometry/Mass Spectrometry. Protein bands in the SDS-PAGE were stained with Coomassie Brilliant Blue (CBB) (Fluka, Buchs, Switzerland). The band of interest was excised from the gel. The gel piece was digested in trypsin solution at 35°C for 20 h for analysis by LC/MS/MS (Aproscience Lifescience Institute, Tokushima, Japan).

Immunoprecipitation. Hippocampal homogenates for Western blottings were used for immunoprecipitation. The antibodies against the proteins of interest were incubated overnight with 50 μl of protein A-Sepharose beads (GE Healthcare, Little Chalfont, Buckinghamshire, UK). To obtain tyrosine-nitrated proteins, anti-nitrotyrosine agarose-conjugated mouse antibody (Millipore) was used. The bead-antibody complexes were incubated overnight with 500 μg of precleared proteins in the corresponding buffers, with the exception that urea lysis buffer does not include dithiothreitol. Immunocomplexes were collected by centrifugation at 13000*g* for 1 min at 4°C and then washed three times with ice-cold PBS. Immunoprecipitated samples were recovered by resuspending in 2× sample loading buffer, immediately fractionated by reducing in 7% SDS-PAGE, and analyzed by Western blotting with the corresponding antibodies.

Histology. Each mouse was anesthetized with diethyl ether and quickly intracardially perfused with physiological saline followed by 4% paraformaldehyde in 100 mM PBS, pH 7.4. The brains were quickly removed, postfixed for 24 h in the same fixative solution, and cryoprotected in a graded 10 to 40% sucrose solution in 100 mM PBS. Coronal sections were cut 20-μm thick using a cryostat (Leica, Wetzlar, Germany) and stained with 0.1% cresyl violet reagent (Wako Pure Chemicals) according to standard procedures. The sections were mounted in fluorescent medium (Dako North America, Inc., Carpinteria, CA), and images of CA1, CA3, and the granular layer of the dentate gyrus of the hippocampus were taken using a Carl Zeiss Axioskop phase-contrast microscope with a cooled CCD camera system (SenSys; Photometrics Ltd., Tucson, AZ). The Nissl-positive neuronal cells were counted using Image J software (version 1.38; National Institutes of Health, Bethesda, MD). The total cell count in per millimeter square was averaged from four sections per animal ($n = 4$) according to previous reports (Nabeshima et al., 1991; Nitta et al., 1997).

Statistical Analysis. The results are expressed as the mean ± S.E. Statistical significance was determined with a one-way analysis of variance followed by the Bonferroni multiple comparisons test. $p < 0.05$ was taken as a significant level of difference.

Results

The Tyrosine Nitration of Proteins Induced by $A\beta_{25-35}$ in the Hippocampus of Mice. Anti-nitrotyrosine mouse antibody detected only a single band of hippocampal proteins at approximately 70 kDa for tyrosine nitration, which induced a potent nitrating agent after the i.c.v. injection of $A\beta_{1-40}$, $A\beta_{25-35}$, and peroxynitrite ($ONOO^-$) (Fig. 2A). Aβ peptides induced extensive nitration of proteins in the hippocampus and impairment of recognition memory, both of which were prevented by UA, a potent scavenger of $ONOO^-$. $ONOO^-$ induced marked tyrosine nitration of proteins in the hippocampus and impairment of recognition memory (Fig. 2, B and C). The intensity of the nitration was inversely associated with the recognition memory in mice (Fig. 2D). The authenticity of nitration was confirmed by the reduction of nitrotyrosine to aminotyrosine with SD in the membrane and by detecting the nitrotyrosine using the same antibody. The absence of this band after SD treatment was regarded as a genuine band for proteins with tyrosine nitration (Fig. 2, E and F). Proteins in SDS-PAGE were stained with CBB, and the 70-kDA protein band was excised for identification (Fig. 2G). The proteins in the excised gel were in-gel-trypsin-digested and subjected to LC/MS/MS, and several proteins were successfully identified (Table 1).

The Identification of the Tyrosine-Nitrated Proteins and the Level of Nitration. The nitration of the identified proteins was examined by applying the immunoprecipitation method. For peptide match scores, HSP70, DRP-2, and NFL were favored for the further study. Because the antibody that was used to detect the nitrated proteins in Western blot analysis could not be used for immunoprecipitation, a specially designed agarose-conjugated mouse anti-nitrotyrosine monoclonal antibody was used. We applied $A\beta_{25-35}$ for the rest of the study, considering its property to produce stronger and stable oxidative damage (Pike et al., 1995) as evidenced in Fig. 2. Immunoprecipitated nitrated-proteins were fractionated by SDS-PAGE and blotted with the antibodies raised against the proteins of interest (Fig. 3A). Intensive